

Review

# MOF-Based Materials for Glucose Detection

Yiling Zhang <sup>†</sup>, Qian Lin <sup>†</sup>, Yiteng Song, Jiaqi Huang, Miaomiao Chen, Runqi Ouyang, Si-Yang Liu <sup>\*†</sup>   
and Zong Dai

Guangdong Provincial Key Laboratory of Sensing Technology and Biomedical Instrument, School of Biomedical Engineering, Shenzhen Campus of Sun Yat-Sen University, Sun Yat-Sen University, Shenzhen 518107, China; zhangyiling27@mail2.sysu.edu.cn (Y.Z.); linq59@mail2.sysu.edu.cn (Q.L.); songyt8@mail2.sysu.edu.cn (Y.S.); huangjq59@mail2.sysu.edu.cn (J.H.); chenmm35@mail2.sysu.edu.cn (M.C.); ouyrq3@mail2.sysu.edu.cn (R.O.); daizong@mail.sysu.edu.cn (Z.D.)

\* Correspondence: liusiyang@mail.sysu.edu.cn

<sup>†</sup> These authors contributed equally to this work.

**Abstract:** Metal–organic frameworks (MOFs), constructed by coordination between metal-containing nodes and organic linkers, are widely used in various fields due to the advantages of tunable pores, diverse functional sites, stable structure, and multi-functionality. It should be noted that MOF-based materials play a major role in glucose detection, serving as a signal transducer or functional substrate for embedding nanoparticles/enzymes. Diabetes is one of the most common and fast-growing diseases worldwide, whose main clinical manifestation is high blood sugar levels. Therefore, accurate, sensitive, and point-of-care glucose detection is necessary. This review orderly introduces general synthetic strategies of MOF-based materials (pristine MOF, nanoparticles, or enzymes-modified MOF and MOF-derived materials) and detection methods (electrochemical and optical methods) for glucose detection. Then, the review refers to the novel MOF-based glucose detection devices (flexible wearable devices and microfluidic chips), which enable non-invasive continuous glucose monitoring or low-cost microscale detection. On the basis of describing the development of glucose sensors based on MOF materials in the past five years, the review presents merits, demerits, and possible improvements of various detection methods.

**Keywords:** metal–organic frameworks (MOFs); glucose detection; synthesis; electrochemical sensor; optical sensor; wearable sensor



**Citation:** Zhang, Y.; Lin, Q.; Song, Y.; Huang, J.; Chen, M.; Ouyang, R.; Liu, S.-Y.; Dai, Z. MOF-Based Materials for Glucose Detection. *Chemosensors* **2023**, *11*, 429. <https://doi.org/10.3390/chemosensors11080429>

Academic Editor: Chung-Wei Kung

Received: 22 June 2023

Revised: 24 July 2023

Accepted: 31 July 2023

Published: 2 August 2023



**Copyright:** © 2023 by the authors. Licensee MDPI, Basel, Switzerland. This article is an open access article distributed under the terms and conditions of the Creative Commons Attribution (CC BY) license (<https://creativecommons.org/licenses/by/4.0/>).

## 1. Introduction

Glucose is an indispensable small molecule for human life, which not only provides energy for the human body but also controls cell activities by regulating the intracellular glucose level. For example, one of the important methods to treat cancer is blocking intracellular glucose uptake, which can effectively inhibit the activity of cancer cells [1,2]. Meanwhile, glucose is also an important intermediate of metabolism. When the blood glucose level deviates from the normal range, serious damage to the human body may be caused, including tissue damage, stroke, renal, heart attack, etc. [3]. Moreover, diabetes, a common metabolic disease, is mainly characterized by high blood glucose levels. The blood glucose disorder also occurs in pancreatic exocrine (pancreatitis, cystic fibrosis, etc.) and endocrine diseases (Cushing syndrome, acromegaly, etc.) [4]. Nowadays, the self-monitoring of blood glucose levels is the most efficient way for the management of diabetes and other related disease [5]. Except for the above-mentioned applications, glucose detection is also applied in artificial taste sensors and quality control of food and drinks [6].

The glucose sensors on the market quantify the glucose by measuring the biochemical reaction products generated from glucose with the catalysis of enzymes, including glucose oxidase-peroxidase (GOD-POD), glucose dehydrogenase (GDH), and hexokinase (HK) [7]. The GOD-POD method is usually utilized in portable glucose meters (finger-prick

blood testing) and self-monitoring blood glucose meters (interstitial fluid detection), which are based on the product ( $H_2O_2$ ) and the electron transfer during the glucose oxidation reaction [8]. The HK method is highly accurate and precise but needs large and expensive equipment, which is commonly used in hospital and laboratory research. In the HK method, the phosphorylation product of glucose catalyzed by hexokinase can react with nicotinamide adenine dinucleotide phosphate ( $NADP^+$ ) under the cascade catalysis of glucose phosphate dehydrogenase (G6PDH) and generate a chemiluminescence signal [9]. Although these methods are widely reported and even commercialized, their sensitivity, stability, and non-invasive detection are still challenged. Consequently, an accurate, selective, stable, and non-invasive glucose detection method is highly demanded. With the advancements in material science, emerging functional materials with superior glucose detection performance have been increasingly reported.

Due to the tunable pores, diverse functional site, high specific surface area, and stable structure, metal–organic frameworks (MOFs), constructed by connecting metal-containing nodes with organic linkers through coordination bonds, have received extensive attention in various detections, especially in glucose detection (Figure 1) [10–14]. MOF-based materials in glucose sensors can be divided into three types, including pristine MOF, modified MOF, and MOF-derived material. Pristine MOF with inherent redox properties that catalyze the reaction of glucose is mostly utilized in non-enzymatic glucose detection. The desired detection properties can be obtained from appropriate ligands and metal ions, and it is also related to the degree of conjugation and coordination of MOF. The modification of MOF with nanoparticles and enzymes can also endow MOF-based materials with catalytic properties and improved detection ability. In addition, after the thermal or solvent treatment, the MOF-derived materials can achieve novel pore structure and detection properties. The detection mechanism of MOF-based glucose sensors can be divided into electrochemical and optical methods based on the types of output signals. The electrochemical detection is based on the redox reaction between glucose with MOF or the modified materials. The optical methods utilize the optical signal produced by the interaction with the glucose and the modified fluorescent probe, enzymes, or MOFs. The preparation strategy (pristine MOF, nanoparticles in/on MOF, enzymes in/on MOF, and MOF-derived materials) and detection mechanism (electrochemical and optical detection) of MOF-based sensors are also inseparable; therefore, this review will introduce MOF-based materials for glucose detection mainly from these two aspects: the preparation strategies and the detection methods.

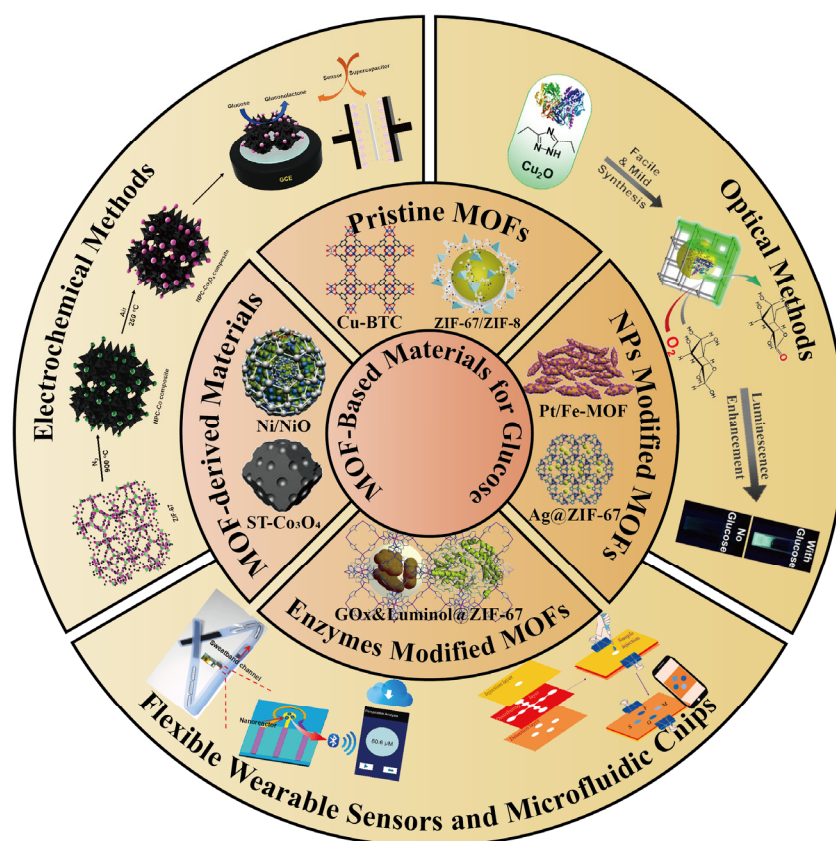


**Figure 1.** Different types of MOF-based materials for glucose detection. Pristine MOFs: Cu-BTC (benzene-1,3,5-tricarboxylate) (reproduced with permission from [15], copyright © 2013, Royal Society of Chemistry), ZIF-67/8 (reproduced with permission from [16], copyright © 2022, Elsevier); NPs modified MOFs: AgNPs@ZIF-67 (reproduced with permission from [17], copyright © 2018, Elsevier), Pt/Fe-MOF (reproduced with permission from [18], copyright © 2021, Springer Nature); Enzymes modified MOFs: GOx&Luminol@ZIF-67 (reproduced with permission from [19], copyright © 2023, Elsevier); MOF-derived materials: Ni/NiO (reproduced with permission from [20], copyright © 2020, Springer Nature), ST-Co<sub>3</sub>O<sub>4</sub> (reproduced with permission from [21], copyright © 2021, John Wiley and Sons). The typical works of electrochemical methods (reproduced with permission from [22], copyright © 2018, Elsevier) and optical methods (reproduced with permission from [23], copyright © 2019, John Wiley and Sons) for glucose detection with MOF-based materials. Furthermore, the flexible wearable sensors (reproduced with permission from [24], copyright © 2022, Elsevier) and microfluidic chips (reproduced with permission from [25], copyright © 2022, Elsevier) for MOF-based glucose detection.

## 2. Synthesis Strategy of MOF-Based Materials

### 2.1. Pristine MOF

The pristine MOF with a large specific surface area and structural diversity is commonly utilized in nonenzymatic electrochemical detection, which avoids restricting detection and storage requirements [26]. In electrochemical detection, the valence of metal ions in pristine MOF is changed, resulting in a redox reaction. The MOF-based electrodes not only have excellent electrocatalytic performance for glucose but also have remarkable selectivity and stability. The pristine MOF used in glucose detection can be divided into single metallic MOF, like Fe [26,27], Co [28], Cu [29,30], and Ni-MOF [31,32], and bimetallic or multivalent metallic MOF. Due to the different ligand coordination abilities, valence states, and ionic radii of the two metals, the substitution of the second metal to the host metal happens, and the crystal structure, morphology, and catalytic properties are changed. On the one hand, the addition of the second metal could improve the catalytic ability and bring other unique properties. On the other hand, the extensive substitution of the

second metal may lead to crystal distortion and structural collapse. The synergism and competition between the two metals improve the bimetallic MOF electrodes and increase the number of structure defects, which endow the electrodes with more binding sites and stronger electrocatalytic performance [33]. Ma et al. synthesized a novel stylophora coral-like furan-based Ni/Co-MOF (Ni/Co-FAMOF) through the simple solvothermal method [34]. Ni/Co-FAMOF, combined with bimetal Ni/Co and furan dicarboxylic acid ligand, has a high specific capacitance, capacity retention rate, and good electrochemical glucose detection performance. The excellent performance of the Ni/Co-FAMOF electrode derived from (1) ligand with rigid furan ring skeleton, which has high molecular stacking properties; (2) bimetal-containing nodes, which combine the high electrocatalytic activity of Ni and oxygen adsorption ability of Co; and (3) unique stylophora coral-like morphology, which greatly increases the active sites on the surface.

### 2.1.1. Hydrothermal/Solvothermal Synthesis

Hydrothermal/solvothermal synthesis is one of the most commonly employed methods to synthesize pristine MOF for glucose detection. Hydrothermal/solvothermal synthesis typically reacts the metal salts and organic ligands in a closed system, such as a Teflon-lined steel autoclave, with water or organic solvent at a relatively high temperature (100–1000 °C) and pressure (1 MPa–1 GPa). The medium provides a favorable reaction environment to promote the generation of desired products, which inhibits the formation of undesirable products. Therefore, hydrothermal/solvothermal synthesis has the advantages of high purity of products, efficiency, simplicity, versatility, and large-scale preparation [35].

The mechanisms of crystal growth by hydrothermal/solvothermal growth are dissolve crystallization and in situ crystallization (Table 1). Dissolve crystallization: the dissolved precursor mixture reaches a subcritical or supercritical state under high temperature and pressure and converts to the final product for the different solubility between product and precursor [36]. Ramaprabhu et al. synthesized copper-terephthalate (CuBDC) MOF by solvothermal method with different time durations [37]. When the reaction time exceeded 6 h, Cu-BDC started agglomerating, and the morphology changed from flat, rod-shaped into a cuboidal solid block-shape with stacked layers, which completely changed after 48 h. The changes in the morphology greatly increased the specific surface area and active sites, which further improved the detection performance in glucose detection.

In situ crystallization: in the presence of precursors (such as graphene, carbon cloth, metal nanoparticles, etc.), MOF crystals are promoted to in situ grown at active sites formed by the dehydration of precursors [38]. As shown in Figure 2A, Yang et al. used the in situ growth method to prepare NiCo-BTC nanosheets on the surface of the precursor carbon cloth (CC) with oxygen-containing functional groups [39]. The application of CC not only improved the distribution of NiCo-BTC and avoided aggregation but also increased the active site to oxidize glucose. The electrochemical performance for glucose detection was further improved, attributing to the positive synergistic effect of bimetal. Wang et al. successfully in situ grew bimetallic CuCo-MOF on nickel foam (NF) through a facile one-pot hydrothermal treatment [40]. With the positive synergistic effect of Co and Cu, CuCo-MOF obtained enhanced sensitivity of electrodes from Co and broadened linear range from Cu. The microflower-like morphological structure further improved electrochemical glucose detection properties.

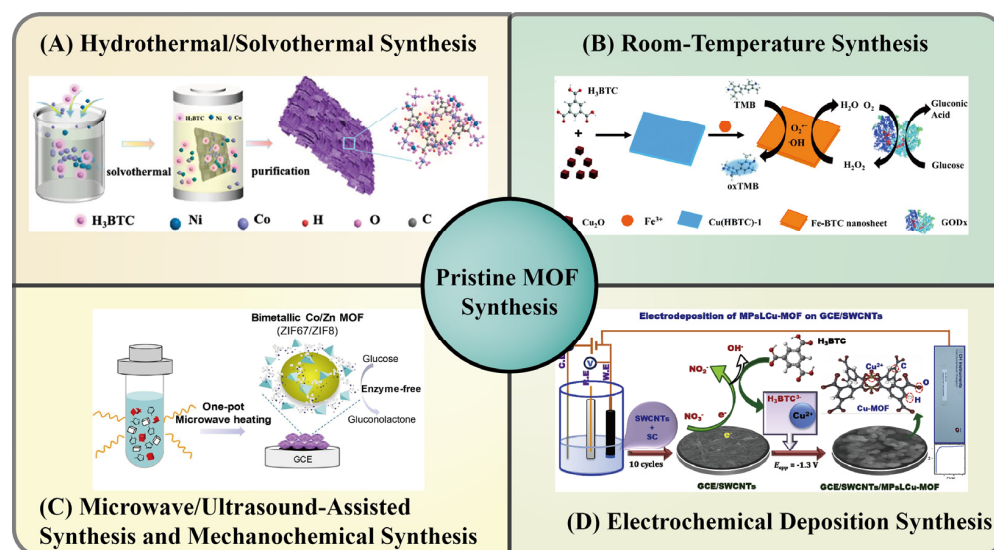


**Figure 2.** Synthesis methods of the pristine MOF. (A) Solvothermal synthesis of NiCo-BTC/CC (reproduced with permission from [39], copyright © 2022, American Chemical Society). (B) Room-temperature synthesis of 2D Fe-BTC (reproduced with permission from [41], copyright © 2013, Royal Society of Chemistry). (C) Microwave-assisted synthesis of ZIF-67/8 (reproduced with permission from [16], copyright © 2022, Elsevier). (D) Electrochemical deposition synthesis of Cu-BTC on SWCNTs/GCE (reproduced with permission from [42], copyright © 2020, Elsevier).

**Table 1.** MOF synthesized by hydrothermal/solvothermal synthesis for glucose detection.

Sample	Solvent	Method	Morphology	Ref
Ni/Co-FAMOF	H <sub>2</sub> O	Dissolve crystallization	Stylophora coral-like	[34]
Co-MOF	ChCl	Dissolve crystallization	Nanoparticles	[43]
Co-BTC	DMF, Ethanol	Dissolve crystallization	Cuboid	[44]
NiCu-MOF	DMF	Dissolve crystallization	Nanosheets	[45]
NiCo-BTC/CC	Ethanol	In situ crystallization	Nanosheets	[39]
Co/Cu-MOF/NF	H <sub>2</sub> O	In situ crystallization	Microflowers	[40]
Ni/Co(HHTP)MOF/CC	H <sub>2</sub> O	In situ crystallization	Thick rods	[46]
CuCo-MOF/CFP	DMF	In situ crystallization	Book-like	[47]

BTC: benzene-1,3,5-tricarboxylate. DMF: N, N-Dimethylformamide. HHTP: triphenylene-2,3,6,7,10,11-hexaol. CFP: carbon fiber paper.

In addition to solvothermal/hydrothermal synthesis, ionothermal synthesis was also applied to synthesize MOFs for glucose detection. Compared with solvothermal/hydrothermal synthesis, which uses water or an organic solution as a solvent, ionothermal synthesis uses ionic liquids as reactants, which could also act as structure-guiding agents and charge-balancing agents. The ionic liquids, which have unique ionic composition, low freezing point, strong solubility, and good electrical conductivity, incubate the ionothermal synthesis with high safety and green environmental protection. Jiao et al. utilized the deep eutectic solvent choline chloride (ChCl) as a solvent to synthesize Co-MOF, [Ch]<sub>2</sub>[Co<sub>3</sub>(BDC)<sub>3</sub>Cl<sub>2</sub>] [43]. The detection performance of the synthesized [Ch]<sub>2</sub>[Co<sub>3</sub>(BDC)<sub>3</sub>Cl<sub>2</sub>] electrode towards glucose is excellent, with a rapid response.

### 2.1.2. Room-Temperature Synthesis

The room-temperature synthesis strategy, which reacts under room temperature and mild conditions, is simple and facile. Moreover, room-temperature synthesis is suitable for industrial large-scale production to eliminate unstable factors, including the heating and pressurization process [48]. Wang et al. prepared an electrode with Co-MOF on CC, which was fabricated by the room-temperature liquid-phase deposition strategy [49]. The room-temperature liquid-phase deposition strategy avoided post-coating procedures with polymeric binders that inevitably reduced the active surface area and the rate of charge

transfer. Furthermore, the ultrathin two-dimensional (2D) Co-MOF nanosheets with well-aligned open-shelled MOF nanoarrays on CC promoted the penetration of electrolytes and the diffusion of small molecules and improved the oxidation efficiency of glucose, which endowed the electrode with excellent catalytic performance. As shown in Figure 2B, Huang et al. synthesized Cu(HBTC) using the room-temperature synthesis strategy, and  $\text{Fe}^{3+}$  ions were added to replace the  $\text{Cu}^{2+}$ , obtaining Fe-BTC with peroxidase activity. The 2D nanosheets of Fe-BTC offered higher diffusion efficiency and more active sites than three-dimensional (3D) bulk crystals, which improved the glucose detection performance [41]. Additionally, NiCo-MOF [50,51], Cu-MOF [52–54], ZIF-67 [55], and other MOFs were also synthesized using the room-temperature synthesis strategy to detect glucose.

### 2.1.3. Microwave/Ultrasound-Assisted Synthesis and Mechanochemical Synthesis

With the assistance of high-energy ultrasonic and electromagnetic waves to increase the reaction energy, respectively, microwave/ultrasound-assisted synthesis has the advantages of high efficiency, rapid reaction, uniform particle morphology, and high phase purity. In microwave-assisted synthesis, the interaction between the electromagnetic field of the microwave and electrons, the precursors which receive the energy from the microwave, are heated uniformly and rapidly to accelerate nucleation and crystal growth [56]. The ultrasound-assisted synthesis is based on the effect of the acoustic cavitation; the bubbles are continuously generated, grown, and collapsed in a hot spot, where the temperature reaches 5000 °C, the pressure is 1000 atm, and the heating/cooling rate is above 1010 K/s, inducing local heating and pressurization. The high temperature and pressure promote the growth of the surrounding crystal nucleus [57]. Compared with traditional hydrothermal/solvothermal synthesis, microwave/ultrasound-assisted synthesis greatly reduces the reaction time, even just in a few minutes. As shown in Figure 2C, Ni et al. used a one-pot, rapid microwave-assisted method to synthesize bimetallic ZIF-67/8 that only needs 20 min [16]. The same method was also used to synthesize Ni-MOF by Sargazi et al. [58]. The synthesized Ni-MOF electrode with a high surface area of 1381 m<sup>2</sup>/g had high sensitivity and accuracy in glucose detection.

Except for microwave/ultrasound-assisted synthesis, mechanochemical synthesis is also used to synthesize MOF-based materials in glucose detection. After applying appropriate mechanical force, the fluidity at the molecular level of the reactants is increased, which results in the breaking of intramolecular bonds and accelerating the chemical reaction [59]. Moreover, mechanochemical synthesis requires no external heat, which is simple, green, and rapid. Lee et al. introduced an innovative rapid agitation-induced synthesis route to synthesize Ni-MOF at 10,000 rpm, which only needs 5 min [60]. The synthesized 2D ultrathin Ni-MOF nanosheet has a good electrocatalytic activity for glucose detection.

### 2.1.4. Electrochemical Deposition Synthesis

The electrochemical deposition method, which deposits MOF directly on the conductive substrates, effectively eliminates the decrease of charge transfer efficiency caused by the use of adhesives, such as Nafion. This strategy has the advantages of mild reaction and easy treatment, which also can effectively eliminate the influence of counter ions [61,62]. Meanwhile, changing the electrolyte and current density can effectively control the shape, size, and distribution of MOF. As shown in Figure 2D, Tominaga et al. electrodeposited three-dimensional (3D) nucleated microparticles like Cu-BTC directly on glassy carbon electrode (GCE) with single-walled carbon nanotubes (SWNTs) [42]. Hosseini et al. formed a crystalline rectangular bar-shape Co-BTC on rGO/GCE by depositing nano-flake  $\text{Co}(\text{OH})_2$  intermediates on rGO/GCE and rapidly converting  $\text{Co}(\text{OH})_2$  to Co-BTC [63]. Compared with the one-step electrochemical deposition method, the multi-step electrochemical deposition method, intermediate deposition, and conversion can more effectively control the growth and distribution of MOF and improve the adhesion of MOF to the electrode.

## 2.2. Nanoparticles-Modified MOF

Compared with pristine MOF, MOF modified with other materials, including nanoparticles (NPs) and enzymes, can achieve diverse functions and properties for glucose detection (Table 2). Most pristine MOF was applied in electrochemical detection, and the choice of metal in MOF is limited to redox metals, such as Fe, Co, Cu, and Ni. Excitingly, the modified MOF broadened the choice of metals, ligands, and detection methods [64]. Because of the pore osmotic adsorption of porous MOF materials and the interaction between functional groups on MOF and NPs (van der Waals force, hydrogen bonding, electrostatic adsorption, etc.), nanoparticles can be stably and uniformly dispersed in the pores of MOF and prevent the aggregation [65]. Hereafter, the synthesis of two types of NP/MOF composites for glucose detection was reviewed (Figure 3).

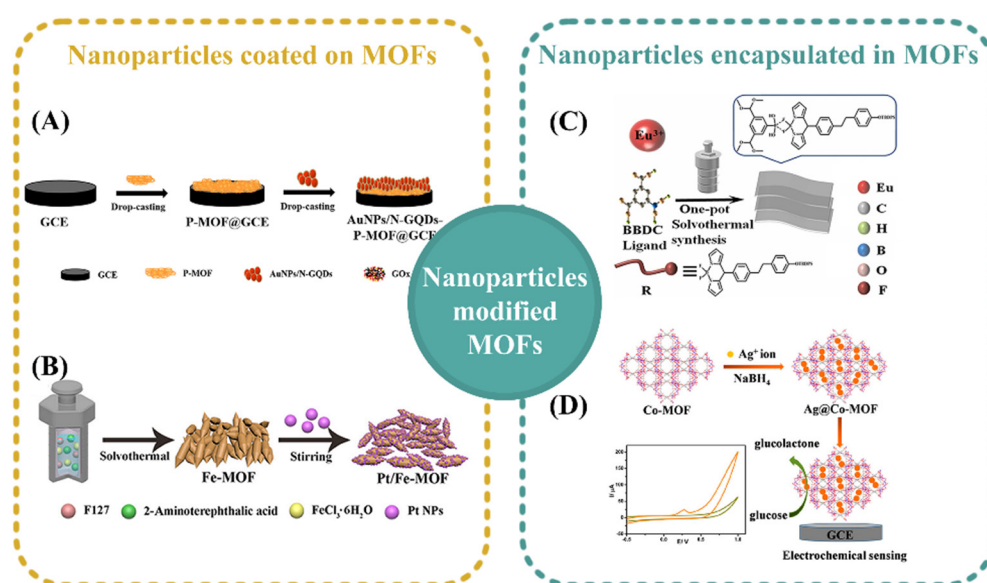


**Figure 3.** The synthesis of NPs-modified MOFs. NPs coated on MOFs: (A) AuNPs/N-GQDs coated on P-MOF as a substrate (reproduced with permission from [66], copyright © 2022, Elsevier); (B) PtNPs coated on Fe-MOF as a catalyst (reproduced with permission from [18], copyright © 2021, Springer Nature). NPs encapsulated in MOFs: (C) BODIPY encapsulated in Eu-MOF by one-pot synthesis (reproduced with permission from [67], copyright © 2022, Elsevier); (D) AgNPs encapsulated in Co-MOF by in situ growth (reproduced with permission from [68], copyright © 2019, American Chemical Society).

### 2.2.1. NPs Coated on MOFs

NPs, including noble metal nanoparticles, metal oxides, quantum dots, etc., were usually used to modify MOFs to improve detection performance [69]. According to the role played by MOFs, NPs-coated MOFs can be divided into two categories: (1) MOFs were applied as substrates to immobilize NPs with catalytic properties. (2) MOFs were used as catalytic materials, and the coated nanoparticles interacted with MOFs to improve the catalytic performance.

#### MOFs as Substrates

The NPs can be absorbed in the pores or on the surface of MOFs, which prevents the aggregation and reduction of the catalyst activity. Meanwhile, MOFs also can promote contact between the active site and the substrate, which is very suitable to be used as the substrate of NPs. As shown in Figure 3A, Wu et al. used the PEI functionalized MOF as the substrate to physically absorb AuNPs/N-GQDs on the surface [66]. PEI-functionalized Fe-MOF provides a large specific surface area for AuNPs/N-GQDs and facilitates the contact between uniformly dispersed active sites and the electrode surface. The enzyme-

linked reaction of AuNPs/N-GQDs with peroxidase mimics (AuNPs) and nitrogen-doped graphene quantum dots (N-GQDs) realized the glucose detection.

#### MOFs as Catalyst

Besides simply being a substrate, MOFs also possess diverse properties, especially catalytic activities, including peroxidase activity, electrocatalytic activity, etc. Thus, MOFs can also be used in glucose detection and the detection performance as catalysts to further improve the detection performance. Lu et al. utilized the coordination between PtNPs and Fe-MOF to stabilize PtNPs on the surface of Fe-MOF (Figure 3B) [18]. The electrons on PtNPs can induct to transfer to Fe, which accelerates the redox cycle of  $\text{Fe}^{3+}/\text{Fe}^{2+}$ , which significantly improves the efficiency of the peroxidase reaction of Fe-MOF. There are many NPs on MOFs synthesized by similar methods, such as N-Co-MOF@PDA-AgNPs [70],  $\alpha$ -CD-rGO/Ni-MOF [71], RhB-CDs@MOF-808 [72], etc.

#### 2.2.2. Nanoparticles Encapsulated in MOFs

Except for coating NPs on the surface of MOFs, encapsulating NPs in MOFs also can be used for glucose detection, including in situ encapsulation and in situ growth [65].

As for the in situ encapsulation method, the NPs are encapsulated in MOFs by adding the pre-synthesized NPs into the mother solutions of MOF, and the MOF crystalizes around the NPs, which act as crystal nuclei [64]. For instance, Bagheri et al. synthesized  $\text{CeO}_2$ @NH<sub>2</sub>-MIL-88B by a room-temperature one-pot strategy to form a colorimetric detection system for glucose detection [25]. The  $\text{CeO}_2$  enhanced the peroxidase activity of NH<sub>2</sub>-MIL-88B, exhibiting faster response speed and stronger colorimetric signal compared to horseradish peroxidase (HRP).

The in situ growth method requires two or more steps for preparation. First, the precursors of NPs, such as metal salts and polymer monomers, are encapsulated or immersed into the pores of MOF. Next, NPs are formed in situ by polymerization or redox reaction [69], generating relatively small NPs with homogeneous distribution and improved stability. Lu et al. in situ polymerized polypyrrole (PPy) in Co-Ni(Fe)-MOF nanosheets to fabricate the Co-Ni(Fe)-MOF/PPy electrode [73]. The  $\text{Fe}^{3+}$  catalyzed the in situ polymerization of PPy, avoiding the addition of additional oxidants and improving the conductivity and electrocatalytic performance of composite electrodes. Wang et al. used the in situ growth method to embed highly conductive and biocompatible AgNPs into Co-MOF (Figure 3D) [68]. The encapsulation of AgNPs enhanced the conductivity and electrocatalytic activity of the Ag@Co-MOF electrode.

**Table 2.** MOFs modified with NPs for glucose detection.

Sample	NPs	Function	Method	Ref
P-MOF	AuNPs/N-GODs	Substrate	Physical adsorption	[66]
UiO-66-NH <sub>2</sub>	PPG@Ru	Substrate	EDC/NHS	[72]
Fe-MOF	PtNPs	Improve performance	Coordinate bonds	[18]
N-Co-MOF@PDA	AgNPs	Improve performance	Surface growth	[70]
Ni-MOF	$\alpha$ CD-rGO	Improve performance	Surface electrodeposition	[71]
Eu-MOF	BODIPY	Improve performance	In situ encapsulation	[67]
NH <sub>2</sub> -MIL-88B	$\text{CeO}_2$	Improve performance	In situ encapsulation	[25]
ZIF-67	Ag@TiO <sub>2</sub>	Improve performance	In situ encapsulation	[74]
CoNi(Fe)-MOF	PPy	Improve performance	In situ polymerization	[73]
ZIF-67	AgNPs	Improve performance	In situ generation	[17]
Cu-TCPP(Fe).	AuNPs	Improve performance	In situ generation	[75]
Co-MOF	CuNPs	Improve performance	In situ generation	[76]

PPG: poly (N-phenylglycine). EDC/NHS: cross-linker. PDA: polydopamine.  $\alpha$ CD-rGO:  $\alpha$ -cyclodextrin functionalized reduced graphene oxide. BODIPY: boron-dipyromethene. TCPP: Fe(III) tetra(4-carboxyphenyl)porphyrin.

### 2.3. Enzymes-Modified MOFs

Compared with nanozymes, nature enzymes have the advantages of high catalytic efficiency and selectivity. However, natural enzymes are easily denaturalized by high temperatures, acid or alkali environments, and organic solvents, which limits their practical application. As shown in Figure 4, MOFs with a high specific surface area and stability are ideal substrates for the immobilization of enzymes, and they can not only protect the structure of enzymes from adverse conditions but also improve the selectivity of enzymes to the substrate through pore confinement [77,78]. The immobilization methods of enzymes on MOFs are summarized in Table 3. Moreover, the fluorescence, magnetism, catalysis, and selective adsorption properties of MOFs can be combined with enzymes to achieve abundant expansive functions.

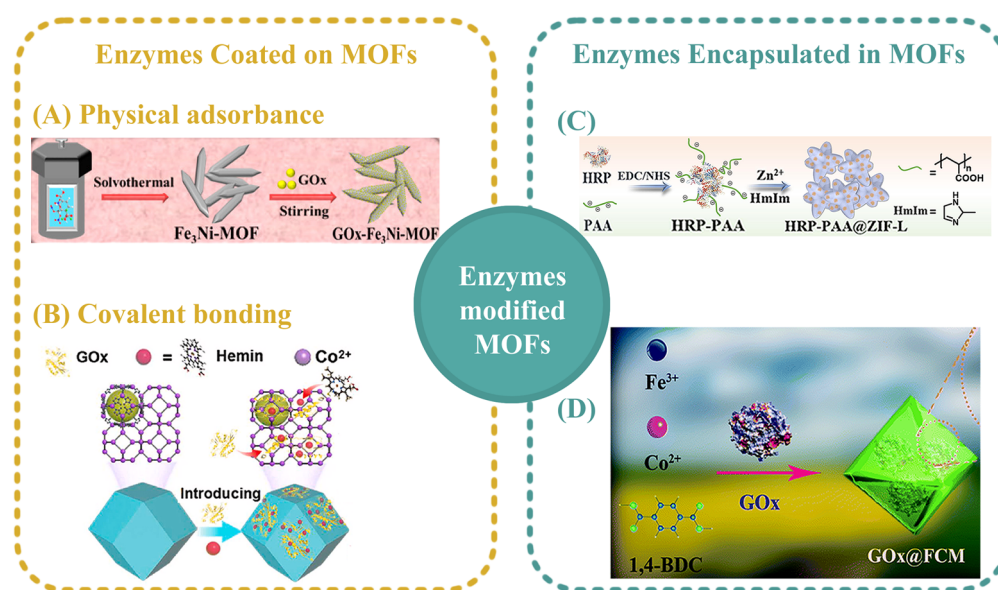


**Figure 4.** The synthesis of enzymes-modified MOFs. Enzymes coated on MOFs: (A) GOx-Fe<sub>3</sub>Ni-MOF by physical adsorption (reproduced with permission from [79], copyright © 2022, American Chemical Society); (B) GOx&Hemin-ZIF-67 by the coordination between the Co<sup>2+</sup> and the carbonyl group of the proteins (reproduced with permission from [24], copyright © 2022, Elsevier). Enzymes encapsulated in MOFs: (C) HRP-PAA@ZIF-L (reproduced with permission from [80], copyright © 2022, Elsevier); (D) GOx@FCM (reproduced with permission from [81], copyright © 2012, Royal Society of Chemistry).

#### 2.3.1. Enzymes Coated on MOFs

Similar to the modification of NPs on the surface of MOFs, enzymes can also be modified on MOFs by physical adsorption and covalent bonding [82]. Wang et al. prepared bimetallic Fe<sub>3</sub>Ni-MOFs by solvothermal synthesis, and glucose oxidase (GOx) was coated on the surface of MOF by simple physical adsorption (Figure 4A) [79]. Fe<sub>3</sub>Ni-MOF can not only protect GOx and improve its stability but also has excellent peroxidase activity, benefiting from the bimetal sites. Zhang et al. also coated hierarchically porous HPPCN-222(Fe) with GOx by physical adsorption [83].

In addition, MOF with abundant functional groups on the surface and pores can also bond with biomolecules through covalent bonding and hydrogen bonding. Kim et al. made use of the pore adsorption of Co-MOF and hydrogen bonding, which formed between the carboxyl functional groups of the enzyme and the imine group of the ligand, 2-methylimidazole (2-MIM), to load GOx on Co-MOF successfully [84].

### 2.3.2. Enzymes Encapsulated in MOFs

In situ encapsulation, by which the enzyme encapsulation and MOF crystallization occur at the same time, requires mild synthesis conditions to maintain the activity of the enzymes [85]. Meanwhile, the selection of MOFs with hydrophilic skeletons and the creation of a suitable enzymatic microenvironment are more beneficial to improve the activity and loading efficiency of the enzyme during in situ encapsulation. Yang et al. enhanced the hydrophilicity of the enzyme microenvironment in ZIF-L by grafting short-chain polyacrylic acid (PAA) onto GOx (Figure 4C) [80]. PAA not only promoted the diffusion of substances by forming mesopores in ZIF-L through competitive coordination but also reduced the influence of interfacial interaction on enzyme conformation.

MOFs with peroxidase activity can also be utilized to construct enzyme-linked reaction systems with GOx, which can reduce the types of encapsulated enzymes and simplify the synthesis. Yu et al. in situ encapsulated GOx in FeCo-MOF with peroxidase activity. The layered structure of MOF, treated with tannic acid, not only protected GOx but also reduced its hindrance to material diffusion (Figure 4D) [81].

**Table 3.** MOFs modified with enzymes for glucose detection.

Sample	Enzymes	Function	Method	Ref
Fe <sub>3</sub> Ni-MOF	GOx	Protection, Nanozyme	Physical adsorption	[79]
HPPCN-222	GOx	Protection, Nanozyme	Physical adsorption	[83]
ZIF-8	GOx, BHb	Protection	MIP	[86]
UiO-66-NH <sub>2</sub>	GOx	Protection	Glutaraldehyde fixation	[72]
NiCu-MOF	GOx	Protection, Nanozyme	Glutaraldehyde fixation	[87]
Co-MOF	GOx	Protection, Nanozyme	Hydrogen bond	[84]
HP-MIL-88B-BA	GOx	Protection, Nanozyme	Specific identification	[88]
Fe-MOF	GOx	Protection, Nanozyme	EDC/NHS	[89]
Co-TCPP(Fe)	GOx	Protection, Nanozyme	EDC/NHS	[90]
dZIF-8	GOx, HRP	Protection	In situ encapsulation	[91]
ZIF-L	PAA-GOx	Protection	In situ encapsulation	[80]
Fe/Co-MOF	GOx	Protection, Nanozyme	In situ encapsulation	[81]
ZIF-67	GOx, HRP	Protection, Nanozyme	In situ encapsulation	[19]

BHb: bovine hemoglobin. MIP: molecular imprinting polymers. HP: hierarchically porous. BA: boronic acid.

### 2.4. MOF-Derived Materials

In order to increase the catalytic rate of the catalyst, MOF-derived materials with large pore structures are synthesized. MOF-derived materials with different functions can be obtained through different treatments (thermal treatment, solvent treatment, etc.), such as metal and metal oxide/hydroxide (pyrolysis), metal sulfide (sulfurization) and metal oxide/carbon composites (carbonization), and so on. The recent related studies were listed out in the Table 4. Due to their outstanding catalytic properties, metal and metallic oxide are widely utilized in glucose detection [92,93]. Nowadays, the traditional synthesis method, including hydrothermal synthesis and electrodeposition, are very sophisticated, but the properties of the synthesized materials still remain to be improved [94]. The metallic materials derived from MOFs can not only retain the morphological and structural characteristics of MOFs precursors but also have the advantages of large specific surface area, abundant active sites, and high porosity [95]. Moreover, MOF-derived materials can obtain additional properties from doped non-metallic elements and effectively avoid the aggregation of particles [96]. In addition, MOF-derived materials have higher stability and response ability than the original neat MOFs by creating atomically active sites, exposing more oxygen vacancy, and increasing the mobility of molecules at the solid/liquid interface, resulting in enhanced glucose detection performance.

#### 2.4.1. Thermal Treatment

MOFs contain both inorganic metal-containing nodes and organic ligands; therefore, they possess not only metallic elements but also various non-metallic elements, such as

C, H, N, O, P, S, etc. In order to obtain the desired MOF-derived materials, the undesired element components should be removed by post-processing. One of the most commonly used methods is thermal treatment at a specific temperature and atmosphere [97]. As shown in Figure 5A, Qin et al. synthesized CuO/C core-shell nanoparticles by calcinating Cu-MOF as sacrificial templates at 400 °C in air [98]. The interaction between the carbon shell and CuO core increased the charge transfer efficiency and the oxygen vacancy content, which endowed the catalytic oxidation capacity of CuO/C for glucose. Fransaer et al. formed Co<sub>3</sub>O<sub>4</sub>-NiO/C composites with a “yolk-albumen-shell” structure (YASNiCo@C) by carbonization of bimetallic CoNi-MOF (Figure 5B) [99]. Furthermore, MOF-derived materials synthesized by pyrolysis also include CuO/NiO-C (Cu/Ni-MOF) [100], CuO (CuBTC) [101], and NiFe<sub>2</sub>O<sub>4</sub> (NiFe-MOF) [102], etc.

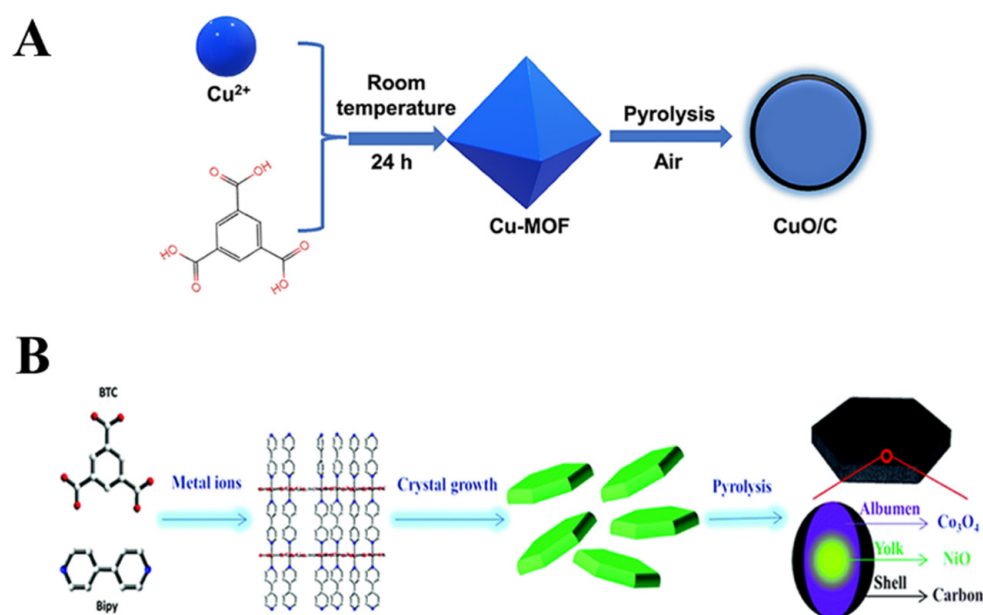


**Figure 5.** (A) The synthesis strategy of CuO/C (reproduced with permission from [98], copyright © 2022, Springer Nature). (B) The synthesis strategy of YASNiCo@C (reproduced with permission from [99], copyright © 2020, Royal Society of Chemistry).

#### 2.4.2. Solvent Treatment

In addition to pyrolysis, MOF-derived materials can also be obtained by solvent treatments, i.e., reacting MOFs with specific etching solutions and obtaining doped metal compounds with special morphology and structure. Jiang et al. prepared nanorod-like porous nickel phosphate NiPO derived from spherical Ni-MOF [103]. The addition of nickel ion controlled the etching degree of Ni-MOF, and the construction of nickel phosphate converted to flower-like, rod-like, and ribbon-like. Liu et al. formed hydrophilic hierarchically-porous nanoflowers (HHNs) by etching hydrophobic ZIF-8 with an organic weak acid, gallic acid (GA) [104]. The synergistic effect of GA with a conjugate rigid plane and free protons combined with nitrogen atoms of ZIF-8 resulted in partial damage of ZIF-8. Therefore, the HHNs kept a 3D hierarchically porous structure consisting of a 2D sheet-like structure and exposed more active sites. With the incorporation of CuNPs into the pores of HHNs, the Cu@HHNs-based electrode obtained superior catalytic activities for glucose electrocatalytic oxidation in glucose detection.

**Table 4.** MOF-derived materials for glucose detection.

Derivative	MOFs	Method	Ref
CuO/NiO-C	Cu/Ni-MOF	Carbonization (430 °C, N <sub>2</sub> )	[100]
Co/MnO@HC	MnCo-MOF-74	Carbonization (900 °C, N <sub>2</sub> )	[105]
NiO/Co <sub>3</sub> O <sub>4</sub> /C	NiCo-MOF	Carbonization (500 °C, Ar <sub>2</sub> )	[106]
Ni/NCNs	Ni-MOF	Pyrolysis (500 °C, N <sub>2</sub> )	[107]
Fe <sub>3</sub> O <sub>4</sub>	Fe-BDC	Pyrolysis (500 °C, N <sub>2</sub> )	[108]
NiO	MOF-74 (Ni)	Pyrolysis (400 °C, N <sub>2</sub> )	[109]
ZnCo <sub>2</sub> O <sub>4</sub>	ZnCo-MOF	Pyrolysis (400 °C, air)	[110]
Ni <sub>3</sub> S <sub>2</sub> @NCNT	Ni-MOF	Carbonization (700 °C, H <sub>2</sub> /Ar <sub>2</sub> ), Sulfurization (Solvothermal)	[111]
E-CuO	Cu-MOF	Etch, Pyrolysis (550 °C, air)	[112]
HHN	ZIF-8	Etch (gallic acid)	[104]
Co-CuS	Cu-Co MOF	Sulfurization (Solvothermal)	[113]
Ni-HHTP	Ni-MOF	Etch (Solvothermal)	[114]

HC: hierarchical carbon. NCNs: nanoporous carbon nanorods. BDC: benzene-1,4-dicarboxylic acid. NCNT: N-doped carbon nanotube. HHTP: 2,3,6,7,10,11-hexahydroxytriphenylene.

### 3. Detection Mechanisms for MOF-Based Glucose Sensors

The previous section introduced four kinds of MOF-based materials for glucose detection. Different types of materials have different functions, and the response signals to glucose are also diverse. Depending on the type of response signal, detection methods can be divided into electrochemical and optical methods. The electrochemical methods include chronoamperometry (CA), linear sweep voltammetry (LSV), cyclic voltammetry (CV), differential pulse voltammetry (DPV), amperometry (AMP), etc. Optical methods include colorimetry, fluorescence (FL), chemiluminescence (CL), surface-enhanced Raman scattering (SERS), etc. In this section, the recent progress on MOF-based electrochemical and optical glucose sensors was reviewed and discussed.

#### 3.1. Electrochemical Methods

Electrochemical detection is a redox-based method where an electric potential is applied between the working and reference electrodes, driving an electrochemical reaction on the surface of the working electrode [115]. This method has gained significant popularity in analytical science due to its high sensitivity, low cost, and ease of operation, making it a powerful tool for various applications [116]. In the following sections, we will discuss recent research advances in electrochemical glucose sensors based on different electrochemical detection methods.

##### 3.1.1. Chronoamperometry

The CA method is a commonly used electrochemical method in which the electric potential of the working electrode is stepped [117]. One of the applications of CA is controlled-potential chronoamperometry. During this process, a constant potential tested from CV measurement is applied to the working electrode, and the current is monitored over time, accompanied by the oxidation or reduction of electrochemically active substances in a solution [118]. Huang et al. successfully electrodeposited MOF (Cu) onto a single-walled carbon nanotube (swnt)-modified gold wire electrode (gwe) to form a composite electrode named swnt-MOF(Cu)@gwe, which has good electrical conductivity (Figure 6A) [119]. Using the chronoamperometric technique to determine glucose, the linear range of modified electrodes was from 1 µM to 3 mM and the limit of detection (LOD) was down to 0.16 µM ( $S/N = 3$ ).

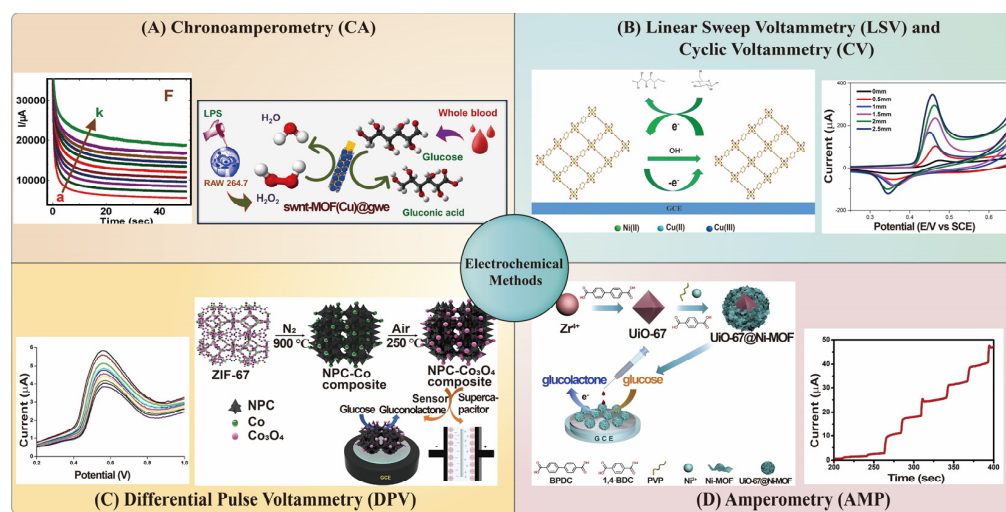


**Figure 6.** (A) Mechanism of glucose oxidation at swnt-MOF(Cu)@gwe and corresponding CA curves for glucose detection (reproduced with permission from [119], copyright © 2023, Elsevier). (B) Mechanism of glucose electrocatalytic oxidation at Ni@Cu-MOF nanocomposite and corresponding CV curves of glucose detection (reproduced with permission from [120], copyright © 2020, Elsevier). (C) Fabrication of NPC-Co<sub>3</sub>O<sub>4</sub> composite and corresponding DPV curves for glucose detection (reproduced with permission from [22], copyright © 2018, Elsevier). (D) Synthesis of core-shell UiO-67@Ni-MOF composites and corresponding AMP curves for glucose detection (reproduced with permission from [121], copyright © 2020, Elsevier).

Although noble metals and their alloys offer a high catalytic activity for glucose oxidation, their high cost and limited availability hinder their widespread use. In contrast, transition metal materials (e.g., Mn, Fe, Co, Ni, and Cu) are more affordable and abundantly available on Earth [122]. In recent years, bimetallic transition materials have received increasing attention due to their unique properties, including versatility, efficient catalytic activity, selectivity, and stability, which often exceed monometallic materials in various applications [123]. Muthurasu et al. used bimetallic MOF to detect glucose. Due to the synergistic effects between metals, bimetallic materials often exhibit enhanced catalytic activity compared to their monometallic counterparts [124]. Finally, they obtained a bimetallic nitrogen-doped carbon nanotube (NCNT) MOF CoCu nanostructure through high-temperature calcination. The CA study demonstrates that the bimetallic NCNT MOF CoCu nanostructure substantially increases the catalytic activity towards glucose. This sensor provides a linear range from 0.05 to 2.5 mM, a sensitivity of  $1027 \mu\text{A} \cdot \text{mM}^{-1} \cdot \text{cm}^{-2}$ , and a LOD of  $0.15 \mu\text{M}$  ( $S/N = 3$ ). The same group also constructed a bimetallic Cu@Ni organic framework electrode, which also used the CA method for sensitive and selective detection of glucose [123]. CA provides a better signal-to-noise ratio in comparison to other amperometric techniques [125], but it shows a relatively slow measurement speed that requires 10 s or longer [126].

### 3.1.2. Linear Sweep Voltammetry and Cyclic Voltammetry

When the potential changes with time, the analyte in a solution will generate a current due to an oxidation or reduction reaction on the electrode surface at the characteristic potential. If a scanning potential changes linearly, it is called LSV; if a scanning potential changes linearly and reverses at a certain time, it is called CV.

Ozacar et al. synthesized a MOF-based composite named GOx-reduced graphene oxide (rGO)/Pt NPs@Zn-MOF-74, where rGO/Pt NPs were deposited on Zn-MOF-74 through  $\pi-\pi$  interactions, and GOx was immobilized on rGO/Pt NPs@Zn-MOF-74 via hydrogen bonds [127]. The porous structure of GOx-rGO/Pt NPs@Zn-MOF-74 allowed the substrate to be easily accessible to GOx, improving the electrochemical response. LSV curves of the electrodes indicated that the modified electrode lowered the detection po-

tential for H<sub>2</sub>O<sub>2</sub> compared to the bare glassy carbon electrode, which oxidized H<sub>2</sub>O<sub>2</sub> only above 0.8 V. Kuang et al. grew the GOx@Cu-MOF packaging structure on the surface of a 3D porous conducting copper foam (CF) electrode by a one-step electrochemically assisted biomimetic mineralization method [128]. In the GOx@Cu-MOF/CF electrode, the embedded GOx catalyzes the conversion of glucose into gluconate and H<sub>2</sub>O<sub>2</sub>, and the H<sub>2</sub>O<sub>2</sub> is immediately electrocatalytically reduced by Cu-MOF, resulting in an increase in the reduction current that is measured by CV. A clear linear relationship can be established between the reduction current and the glucose concentration in the concentration range of 0–6 mM. Zhao et al. successfully prepared a nickel-modified Cu-based MOF nanocomposite electrode (Ni@Cu-MOF) as an electrochemical detector for glucose (Figure 6B), with a sensitivity of 1703.33  $\mu\text{A mM}^{-1} \text{cm}^{-2}$ , a linear range between 5 and 2500  $\mu\text{M}$ , and a LOD of 1.67  $\mu\text{M}$  ( $S/N = 3$ ) [120]. However, CV is not an ideal technique for quantitative analysis because the limits of detection and quantification are higher than those of other types of voltammetry [129].

### 3.1.3. Differential Pulse Voltammetry

DPV is a technique involving the application of an amplitude potential pulse to a linear ramp potential [130]. The current is measured before the potential pulse and at the end of the pulse, and the difference between the two currents is recorded as the response [117]. Generally, pulsed techniques (e.g., DPV) are more responsive than linear scanning methods because the capacitive current is minimized, and CV is more commonly used for exploratory analysis [130].

Han et al. developed the nanoporous carbon and cobalt oxide (NPC-Co<sub>3</sub>O<sub>4</sub>) composite through the heat treatment of a MOF precursor, ZIF-67 (Figure 6C) [22]. DPV analysis of NPC-Co<sub>3</sub>O<sub>4</sub>/GCE with different glucose concentrations was performed at a scan rate of 0.1 V s<sup>-1</sup> and a given potential range of 0.2–1.0 V in 0.1 M KOH. The differential pulse voltammetry response of NPC-Co<sub>3</sub>O<sub>4</sub>/GCE has a linear relationship with the glucose concentration. The sensor enables glucose detection in the concentration range from  $5 \times 10^{-12}$  to  $2.05 \times 10^{-10}$  M and a LOD of 2 pM ( $S/N = 3$ ). It is worth noting that the sensitivity reaches up to 0.14  $\mu\text{A pM}^{-1} \text{cm}^{-2}$ .

Wang et al. grew Cu-trimesic acid (Cu-BTC) MOFs on 3D-macroporous carbon (KSCs) electrodeposited Au NPs on the integrated electrode and then fixed GOx by a Au-S bond. GOD/AuNPs/Cu-BTC MOFs/3D-KSCs were obtained to construct a proportional electrochemical glucose biosensor [131]. Cu-BTC MOF can catalyze glucose oxidation and convert Cu(II) to Cu(I), which enhances the reduction peak of Cu(I) when glucose is added. The DPV response of the O<sub>2</sub> reduction peak current also decreases with the addition of glucose. In order to obtain good selectivity and reproducibility,  $j_{\text{O}_2}/j_{\text{Cu-BTC}}$  was used as the response signal. The sensor enables glucose detection in the concentration range from 44.9  $\mu\text{M}$  to 19 mM and a LOD of 14.77  $\mu\text{M}$  ( $S/N = 3$ ). Ramaprabhu et al. fabricated a copper terephthalate (CuBDC) MOF-modified GCE to construct a non-enzymatic glucose biosensor with a sensitivity of 37.09  $\mu\text{A } \mu\text{M}^{-1} \text{cm}^{-2}$  and a LOD of 0.077  $\mu\text{M}$  ( $S/N = 3$ ) [37]. Compared with the CV technique, the DPV technique displays lower signal background and better sensitivity, resulting in higher resolution at lower concentrations of an analyte [84].

### 3.1.4. Amperometry

AMP has become a commonly used detection method. In 1956, Clark developed the first bio-amperometric sensor for measuring dissolved O<sub>2</sub> in the blood consumed in an enzymatic reaction catalyzed by GOx [132]. AMP involves applying a constant reduction or oxidation potential on the working electrode and then measuring the resulting steady-state current [133].

ZIF-67-derived materials are currently used as efficient catalysts for sensors such as glucose, 4-nitrophenol (4-NP) [134], acetaminophen [2], SO<sub>2</sub> [135], and so on. Ruan et al. synthesized a novel N-doped carbon dodecahedron embedded with Co nanoparticles (Co@NCD) by pyrolyzing ZIF-67 in a reductive atmosphere [136]. ZIF-67-derived electro-

catalysts obtained from high-temperature carbonization have improved conductivity, large surface area, and active non-precious Co and N-doped carbon heterojunctions. By using Co@NCD/GCE to detect glucose, two linear ranges were obtained from current–time curves; one was 0.0002–1.0 mM with a sensitivity of  $125 \mu\text{A mM}^{-1} \text{cm}^{-2}$  and the other was 1.0–12.0 mM with a sensitivity of  $23 \mu\text{A mM}^{-1} \text{cm}^{-2}$ . The LOD was calculated to be  $0.11 \mu\text{M}$  ( $S/N = 3$ ). Aside from that, Yin et al. prepared Au@NiCo LDH via etching ZIF-67 and reducing  $\text{HAuCl}_4$  at a high temperature to construct glucose-sensing electrodes with a sensitivity of  $864.7 \mu\text{A mM}^{-1} \text{cm}^{-2}$  and a LOD of  $0.028 \mu\text{M}$  ( $S/N = 3$ ) [137].

The use of core-shell MOF@MOF materials offers several advantages by combining the chemical, physical, and structural properties of both MOFs, leading to unexpected synergistic effects [138]. Wang et al. first synthesized the core-shell UiO-67@Ni-MOF material [121]. The composite material was synthesized by an internal extended growth method under polyvinylpyrrolidone (PVP) regulation. The pre-prepared UiO-67 was used as the growth core of shell Ni-MOF (Figure 6D). In this study, UiO-67 was selected for its expansive specific surface area and good conductivity, which facilitated efficient electron transfer within the UiO-67@Ni-MOF composite. On the other hand, Ni-MOF exhibited excellent electrochemical activity for glucose oxidation, rendering it an ideal electrocatalytic material. The findings demonstrated that the UiO-67@Ni-MOF composites displayed significantly enhanced electrocatalytic activity for glucose oxidation compared to the individual UiO-67 and Ni-MOF structures.  $\text{Ni}^{2+}$  from Ni-MOF is oxidized to  $\text{Ni}^{3+}$  in the  $-0.43 \text{ V}$  alkaline electrolyte.  $\text{Ni}^{3+}$  then oxidizes glucose molecules at a voltage of  $0.5 \text{ V}$  and produces glucolactone. AMP curves show that the sensor has a fast response ( $<5 \text{ s}$ ), wide linear range ( $5 \mu\text{M}$ – $3.9 \text{ mM}$ ), and low LOD ( $0.98 \mu\text{M}$ ,  $S/N = 3$ ). It has good reproducibility ( $\text{RSD} = 1.1\%$ ), repeatability ( $\text{RSD} = 1.9\%$ ), and long-term stability. It should be noted that the sensitivity and selectivity of the amperometry method are influenced by many factors, such as electrode material, electrolyte solution, temperature, oxygen, etc., and therefore need to be optimized and controlled according to the actual situation.

In addition to being classified by the electrochemical detection method, common electrochemical glucose sensors can also be divided into two types: enzymatic and non-enzymatic sensors (Tables 5 and 6). The glucose biosensor based on enzyme promotion is based on the specific reaction between glucose and active enzymes, which causes the change of an electrical signal so as to realize the detection of glucose. The electrical signals in enzymatic sensors can be generated through various processes, including  $\text{O}_2$  consumption, electrooxidation of  $\text{H}_2\text{O}_2$ , electroreduction of  $\text{H}_2\text{O}_2$ , and oxidation of  $\text{H}_2\text{O}_2$  by peroxidase [139]. However, enzymatic sensors may be affected by several factors, such as pH, temperature, and the presence of detergents [140]. Enzyme-free electrochemical sensors, in contrast to active enzyme-based sensors, utilize substances with glucose catalytic activity directly at the electrode to oxidize glucose. MOF-based materials have been shown to exhibit high electrocatalytic activity [141]. The presence of  $\text{OH}^-$  ions on the electrode surface increases the local pH, creating an alkaline microenvironment that enhances glucose oxidation [37]. This process involves the catalytic oxidation of glucose to gluconolactone, followed by further hydrolysis to gluconic acid. The porous structures and large active surface area of MOF-based materials significantly enhance their analytical performance [137]. Moreover, unique morphologies of MOF-based materials expose more active sites, thereby increasing the contact area with glucose and facilitating faster charge transfer. Additionally, incorporating mixed-valence metal ions or organic ligands into the MOF structure can further enhance the conductivity, catalytic activity, and, therefore, the detection performance of MOF-based materials [142].

**Table 5.** MOF-based non-enzymatic electrochemical glucose sensors.

Electrode Material	Electrochemical Method	Electrolyte	Linear Range ( $\mu\text{M}$ )	LOD ( $\mu\text{M}$ )	Sensitivity ( $\mu\text{A mM}^{-1} \text{cm}^{-2}$ )	Ref
Ni-MOF	CA	0.1 M NaOH	10–2000	1.16	3.03	[143]
Ni <sub>3</sub> (HITP) <sub>2</sub> MOF	CV	0.1 M KOH	0–10,000	–	–	[144]
Ni-MOFN	AMP	0.1 M KOH	25–3150	0.6	402.3	[60]
r-NiPO	AMP	0.1 M NaOH	1–3	1	3169	[103]
NiO/Co <sub>3</sub> O <sub>4</sub> /C	AMP	0.1 M NaOH	0.2–10,000	0.045	2820	[106]
Ni/Co-FAMOF	AMP	1 M KOH	6–1004	2	366	[34]
Ni/Co(HHTP) MOF/CC	AMP	0.1 M NaOH	0.3–2312	0.1	3250	[46]
74(NiO)@NiCo LDH	AMP	1 M KOH	10–1100, 1500–9000	0.278	1699	[109]
NiCu-MOF-6	AMP	0.1 M NaOH	20–4930	15	1832	[45]
Ni@Cu-MOF	CV	0.1 M NaOH	5–2500	1.67	1703.33	[120]
NiCoBP-Br	AMP	0.1 M NaOH	0.5–6065.5	0.0665	1755.51	[47]
Ni-Co MOF/Ag/rGO/PU	AMP	0.1 M NaOH	10–660	3.28	425.9	[140]
YASNiCo@C bimetallic	AMP	0.1 M NaOH	5–5000	0.75	1964	[99]
Cu@Ni organic framework	CA	0.1 M NaOH	0–5000	0.4	496	[123]
UiO-67@Ni-MOF	AMP	0.1 M NaOH	5–3900	0.98	–	[121]
Cu-MOF	DPV	0.01 M NaOH	0.06–5000	0.01	89	[145]
CuBDC12E	DPV	0.02 M PBS (pH 7.4)	0–2000	0.077	37,090	[37]
Cu-MOF/CF	AMP	0.1 M NaOH	1–950	0.076	30,030	[146]
CuO nanorod	CA	0.1 M NaOH	up to 1250	1	1523.5	[147]
swnt-MOF(Cu)@gwe	CA	0.1 M NaOH	1–3000	0.16	–	[119]
CuO/C	AMP	0.1 M NaOH	5–25,325	1	244.71	[98]
Cu <sub>2</sub> (NDC) <sub>2</sub> /PDHP	AMP	electrolyte-simulated sweat	5–1775	2	1690	[148]
CuO polyhedrons/CC	AMP	0.1 M NaOH	0.5–800	0.46	13,575	[15]
Cu@Co-MOF bimetallic	AMP	0.01 M NaOH	5–400	1.6	282.89	[76]
NCNT MOF CoCu nanostructure	CA	0.1 M NaOH	50–2500	0.15	1027	[124]
E-NiCo-BTC MOF	AMP	0.1 M NaOH	1–1780	0.187	1789	[149]
NPC-Co <sub>3</sub> O <sub>4</sub>	DPV	0.1 M KOH	$10^{-6}$ – $2.05 \times 10^{-4}$	$2 \times 10^{-6}$	$0.14 \mu\text{A pM}^{-1} \text{cm}^{-2}$	[22]
Co-MOF	CA	0.01 M NaOH	5–900	1.6	169	[150]
Co@NCD	AMP	0.1 M NaOH	0.2–12,000	0.11	125.23	[136]
Au@NiCo LDH	AMP	1.0 M NaOH	5–12,000	0.028	864.7	[137]
Co/MnO@HC	AMP	0.1 M NaOH	50–900, 1900–6900	1.31	233.8	[105]

HITP: (2,3,6,7,10,11-hexaiminotriphenylene)<sub>2</sub>. MOFNs: MOF nanosheets. r-NiPO: nanorod-like nickel phosphate. LDH: layered double hydroxides. BP: 4-bromopyridine. NDC: naphthalenedicarboxylic. PDHP: pencil drawing hydrophobic paper. E-NiCo-BTC: nickel-cobalt-benzene tricarboxylic acid.

**Table 6.** MOF-based enzymatic electrochemical glucose sensors.

Electrode Material	Electrochemical Method	Mechanism	pH	Linear Range ( $\mu\text{M}$ )	LOD ( $\mu\text{M}$ )	Sensitivity ( $\mu\text{A mM}^{-1} \text{cm}^{-2}$ )	Ref
PDA-GOx-HKUST-1-MWCNTs/Pt/Au	AMP	electrooxidation of H <sub>2</sub> O <sub>2</sub>	7.0	5–7050	0.12	178	[151]
GOD-GA-Ni/Cu-MOFs-FET	AMP	electrooxidation of H <sub>2</sub> O <sub>2</sub>	7.4	1–100	0.51	26.05	[87]
rGO/Pt NPs@Zn-MOF-74	LSV	electrooxidation of H <sub>2</sub> O <sub>2</sub>	7.4	6–6000	1.8	64.51	[127]
GOx-AuNPs/N-GQDs-P-MOF@GCE	AMP	electroreduction of H <sub>2</sub> O <sub>2</sub>	4.0	2–10, 20–3000	0.7	1512.4	[66]

**Table 6.** *Cont.*

Electrode Material	Electrochemical Method	Mechanism	pH	Linear Range ( $\mu\text{M}$ )	LOD ( $\mu\text{M}$ )	Sensitivity ( $\mu\text{A mM}^{-1} \text{cm}^{-2}$ )	Ref
GOx/Hemin@NC-ZIF	AMP	oxidation of $\text{H}_2\text{O}_2$ by peroxidase	7.2	0–20,000	10	–	[24]
GOx@Cu-MOF/CF	CV	electroreduction of $\text{H}_2\text{O}_2$	7.4	0–6000	–	–	[128]
GOD/AuNPs/Cu-BTC/3D-KSCs	DPV	$\text{O}_2$ depletion monitoring	7.0	44.9–4000, 4000–19,000	14.77	–	[131]

MWCNTs: multi-walled carbon nanotubes. GA: glutaraldehyde. FET: field-effect transistor.

### 3.2. Optical Methods

Optical methods for sensing glucose have been extensively studied and developed, such as colorimetry, FL, CL, SERS, etc. The optical glucose sensors based on MOF-based materials provide a visualized and cost-effective way to measure glucose concentrations compared to electrochemical glucose sensors that need relatively expensive and complicated instruments, as well as being prone to interferences [152]. However, the long-term stability and reusability of MOF-based optical glucose sensors are the major challenges for future applications. Hereafter, some typical and important optical glucose sensors are introduced and classified into colorimetry, FL, CL, and SERS-based methods (Table 7).

**Table 7.** MOF-based optical glucose sensors.

Materials	Detection Method	Linear Range ( $\mu\text{M}$ )	LOD ( $\mu\text{M}$ )	Ref
dZIF-8 BH	colorimetry	50–4000	–	[91]
G&L@ZIF@Paper	colorimetry	200–2000	120	[19]
GOx/Hemin@NC-ZIF	colorimetry	1000–20,000	10	[24]
Aga/GOD@Cu-hemin MOF/TMB	colorimetry	30–800	10	[49]
GOx@FCM-TA	colorimetry	5–750	0.94	[81]
$\text{Fe}_3\text{Ni}$ -MOF	colorimetry	2–1000	1	[79]
5R@Eu-MOF	FL	0–6	0.00692	[67]
Ni-MOF	FL	8–30	4	[153]
Pt/Fe-MOF	colorimetry	3900–6400	2.3	[18]
MOF@GOx@BHb-MIPs	colorimetry	0.5–20	0.4	[86]
GOx@MOF-545(Fe)	colorimetry	0.5–20	0.28	[154]
GOx@MAF-2	CL	20–200, 500–30,000	1.4	[23]
$\text{Cu}(\text{bpy})_2(\text{OTf})_2$ nanosheets	FL	10–1000	0.41	[155]
In-aip nanosheets	FL	0–160	0.87	[156]
boric-acid Eu-MOF	FL	0.1–4	0.0643	[157]
Co-TCPP(Fe)@Luminol@GOD	CL	0.177–30.53	0.0592	[90]
Co-MOF	CL	0.04–8	0.012	[158]
AuNPs/Cu-TCPP(Fe)	SERS	160–8000	3.9	[75]
MBs@MIL-100(Fe)@Ag	SERS	20–1000	15.95	[159]
Ag NPs/UiO-66- $\text{NH}_2$	FL	1–200	0.5	[160]
MOF-235/ $\beta$ -CD	CL	0.01–3	0.01	[23]
ficin@MOF	colorimetry	1–140	0.12	[161]
GOx@Zr-PCN-222 (Fe)	colorimetry	0–5000	250	[162]
$\text{CeO}_2$ @ $\text{NH}_2$ -MIL-88B(Fe)	colorimetry	200–15,000	80	[25]

Aga: agarose hydrogels. FCM: Fe/Co-MOF. R: BODIPY. bpy: 4,4-bipyridine. OTf: trifluoromethanesulfonate. aip: aminoisophthalic.

### 3.2.1. Colorimetry

Colorimetry is a fast and effective method for analyzing colored solutions or any colored substances. It is usually measured using a spectrophotometer. The need for point-of-care tests (POCT) has led to the invention of paper-based colorimetric methods, smartphone-based analyses, etc., in the last two decades [163]. The advantages of colorimetry are the convenience of use, high sensitivity, and satisfactory repeatability.

Wang et al. focused on the development of bimetal–organic frameworks ( $\text{Fe}_x\text{Ni}_y\text{-MOF}$ ) as catalysts with peroxidase-like activity (Figure 7A) [79]. By introducing nickel (Ni) into the framework, they achieved enhanced redox capacity and accelerated electron transfer between TMB and  $\text{H}_2\text{O}_2$ . The improved conversion efficiency between  $\text{Fe}^{3+}$  and  $\text{Fe}^{2+}$  ions, coupled with the promotion of  $\cdot\text{OH}$  generation, led to a significant increase in peroxidase-like activity. Based on the excellent activity of  $\text{Fe}_3\text{Ni-MOF}$ , one-step colorimetric detection of glucose is achieved by immobilizing GOx on  $\text{Fe}_3\text{Ni-MOF}$  through physical adsorption. The linear range of the glucose biosensor is 2–1000  $\mu\text{M}$ , and the detection limit is 1  $\mu\text{M}$  ( $S/N = 3$ ).

Moving on to Chen et al.'s work, they presented a biohybrid hydrogel system encapsulating GOx and HRP in a morphology-adjusted defective ZIF biohybrid hydrogel (dZIF-8 BH) [91]. This unique system utilized the biocatalytic cascade involving the conversion of glucose into gluconic acid and  $\text{H}_2\text{O}_2$  by GOx. The generated  $\text{H}_2\text{O}_2$  further oxidized ABTS (single molecule 2,2'-azino-azobis(3-ethylbenzothiazoline-6-sulfonic acid)) into ABTS+ through the peroxidase-like activity of HRP (Figure 7B). The encapsulation within the hydrogel not only provided a stable and confined microenvironment for enzymatic reactions but also facilitated the accumulation of catalytic products, resulting in a stronger color signal for glucose detection. Moreover, the integration of a smartphone with the biosensor opens up the possibility of point-of-care diagnostics and remote monitoring of glucose levels. The dZIF-8 BH portable biosensor provides a glucose detection range from 0.05 to 4 mM. Further, Song et al. developed an integrated agarose-based hydrogel film (Aga/GOD@Cu-hemin MOF/TMB) with a linear range from 30  $\mu\text{M}$  to 0.8 mM and a LOD of 0.01 mM ( $S/N = 3$ ) [49]. Liu et al. encapsulated GOx and luminol in ZIF-67 to form the GOx&luminol@ZIF-67@Paper (G&L@ZIF@Paper) chip (Figure 7C) [19]. The G&L@ZIF@Paper could achieve highly sensitive and specific measurements for glucose with a linear range from 0.2 to 2 mM and a limit of detection of 0.12 mM ( $S/N = 3$ ). The combination of one-pot synthesis and one-pot detection greatly improved the convenience of detection and the possibility of subsequent industrialization. Besides these advantages, the unevenness of color, susceptibility to interference, and relatively low sensitivity of the colorimetric method still need to be improved in order to achieve sensitive and accurate quantification detection of glucose.

### 3.2.2. Fluorescence and Chemiluminescence

Fluorescence (FL), a form of photoluminescence (PL), widely exists in gas, liquid, and solid chemical systems. This method involves the absorption and re-emission of photons by materials, where electrons absorb photons, transition to higher energy levels, and return to the ground state while emitting photons [164]. The FL method has emerged as a powerful tool in qualitative and quantitative analysis due to its rapid detection, reproducibility, high sensitivity, and selectivity.

Among FL sensors, single-emission fluorescence probes encounter challenges related to probe concentration changes, sample light scattering, excitation light fluctuations, and emission collection efficiency [165]. To address these limitations, researchers have turned to dual-emission ratio fluorescence probes, offering higher resolution and improved visualization. For example, Yin et al. developed a ratiometric fluorescence probe using Eu-MOF hollow spheres, exhibiting dual emissions at 370 nm and 623 nm, respectively (Figure 8A) [157]. This probe showed sensitive responses to glucose concentration changes through interactions with the boric acid group and  $\text{H}_2\text{O}_2$ , enabling glucose detection within the range from 0.1  $\mu\text{M}$  to 4  $\mu\text{M}$  with a LOD of 0.0643  $\mu\text{M}$  ( $S/N = 3$ ). In addition, an increase

(on) of one signal (354 nm) and a decrease (off) of the other (624 nm) caused the solution color to change from bright red to blue. Similarly, Ke et al. crafted a ratiometric fluorescence sensor by grafting an R photosensitizer on Eu-MOFs, enabling the detection of  $F^-$ ,  $H_2O_2$ , and glucose in water solutions and living cells [67].

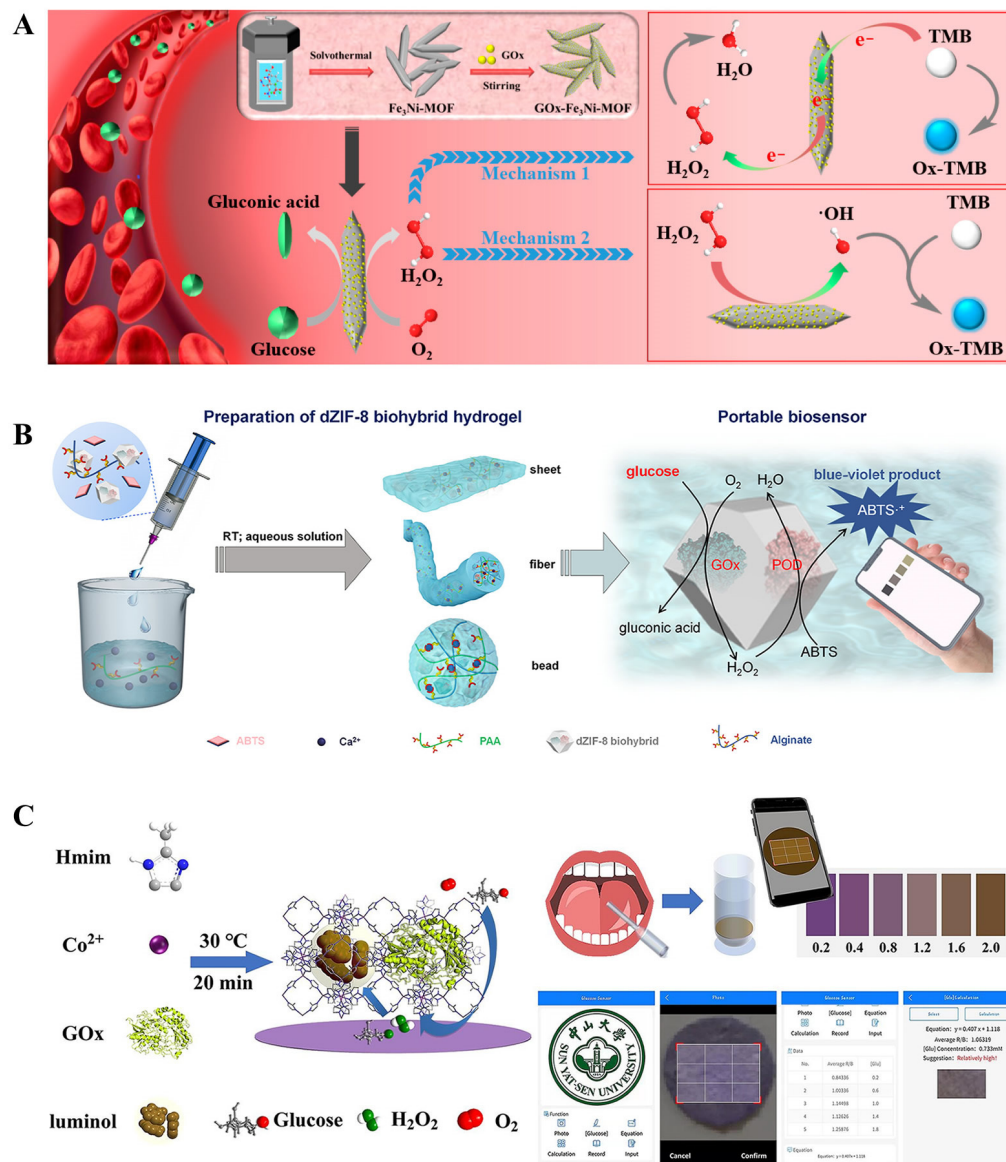


**Figure 7.** (A) Schematic diagram of the synthesis of  $Fe_3Ni$ -MOF/GOx and the reaction mechanism for the cascade oxidation of glucose (reproduced with permission from [79], copyright © 2022, American Chemical Society). (B) Schematic representation of the preparation of dZIF-8 BH and the colorimetric sensing mechanism based on the biocatalytic cascade of dZIFs BH (reproduced with permission from [91], copyright © 2022, American Chemical Society). (C) Schematic illustration of the principle of glucose detection by G&L@ZIF@Paper and the step-by-step flow for detecting glucose in saliva (reproduced with permission from [19], copyright © 2023, Elsevier).

Despite the potential of MOF-based FL sensors, their limited water stability has hindered widespread use. To overcome this challenge, Wang et al. utilized UiO-66- $NH_2$ , known for its excellent stability in water and organic solvents, to design a dual-emission ratiometric fluorescence probe based on the inner filter effect (IFE) for glucose and cholesterol detection (Figure 8B) [160]. In the presence of GOx, glucose is converted to  $H_2O_2$ , which etches Ag NPs into silver ions ( $Ag^+$ ), leading to fluorescent 2,3-diaminophenazine (DAP)

generation from *o*-Phenylenediamine (OPD). The emission spectrum of Ag NPs/UiO-66-NH<sub>2</sub> and the excitation spectrum of DAP produce an effective overlap. The fluorescence intensity ratio ( $F_{555\text{ nm}}/F_{425\text{ nm}}$ ) increases with the target concentration, and the color of the solution changes from blue to yellow-green, enabling higher resolution color variance and better visualization. Furthermore, the reaction reagent is integrated into filter paper, creating a user-friendly test paper that reads RGB values using a smartphone-based portable platform.

Dai et al. introduced a novel concept by combining a responsive MOF with a MOF-enzyme composite, creating a multifunctional “all-in-one” particle that incorporates both catalytic and luminescence capabilities [23]. They successfully encapsulated GOx molecules within the O<sub>2</sub>-sensitive, luminescent Cu<sup>I</sup> triazolate MOF (MAF-2), named GOx@MAF-2 (Figure 8C). This innovative composite offers a noble metal-free solution and provides a single particle with diverse functionalities. The increasing concentration of glucose accelerated the consumption of dissolved oxygen, resulting in the enhanced luminescence intensity of GOx@MAF-2 suspension. The luminescence intensity of the suspension shows good linearity with the logarithmic concentration of glucose in the ranges of 20–200 and 500–30,000 μM, and the detection limit is approximately 1.4 μM ( $S/N = 3$ ).

The difference between CL and FL is that CL is a luminescence phenomenon in which the outer electrons of a molecule absorb the energy of a chemical reaction and are in an excited state, and return to the ground state by a radiative leap [166]. CL reaction involves two key steps, namely chemical excitation and luminescence. The CL reaction between luminol and H<sub>2</sub>O<sub>2</sub> is generally slow and inefficient, but the reaction rate can be greatly enhanced when there are certain catalysts. CL analysis possesses the advantage of high sensitivity, fast responsibility, easy operation, inexpensive instrumentation, low background signal, and so on [158].

In 2018, Huang et al. successfully prepared β-Cyclodextrin functionalization of the metal–organic framework MOF-235 [23]. Due to the synergistic interaction between β-CD and MOF-235, the MOF-235/β-CD hybrid exhibited high catalytic activity on the luminol-H<sub>2</sub>O<sub>2</sub> system. Compared to the luminol-H<sub>2</sub>O<sub>2</sub> system, the CL response of the system using MOFs was enhanced more than 30 times, resulting in much lower detection limits for H<sub>2</sub>O<sub>2</sub> and glucose (5 nM and 10 nM, respectively) (Figure 8D). Following in 2019, Zhang et al. synthesized a 2D-MOF nanosheet with peroxidase activity and sequentially labeled luminol and GOx on the 2D-MOF nanosheet to obtain a simple CL-functionalized glucose sensor (Co-TCPP(Fe)@Luminol@GOD) (Figure 8E) [90]. When GOx oxidizes glucose to produce gluconic acid and H<sub>2</sub>O<sub>2</sub>, 2D-MOF can catalyze the decomposition of H<sub>2</sub>O<sub>2</sub>, further oxidize luminol to generate a strong CL response, and finally realize the rapid detection of glucose with a LOD of 10.667 μg/L (~0.0592 μM).

All in all, future research is likely to focus on enhancing the water stability, dispersibility in solvents, and fluorescence performance of MOF-based FL and CL sensors under real-time environments (pressure, temperature, and mechanical stress) through improved synthetic strategies.

### 3.2.3. Surface-Enhanced Raman Scattering

SERS is a sensitive analytical technique that can significantly enhance the Raman signal of molecules adsorbed on the surface of precious metal nanomaterials by either electromagnetic enhancement (EM) or chemical enhancement (CM) mechanisms [167]. By introducing MOFs, there are two main factors that improve the stability of the SERS substrates: firstly, the large specific surface area of MOFs provides an abundance of sites to capture target analytes; secondly, the MOFs shell protects the NPs from oxidation and corrosion [168]. Thus, the research on the synthesis of SERS substrates based on MOFs has become more and more active in recent times.

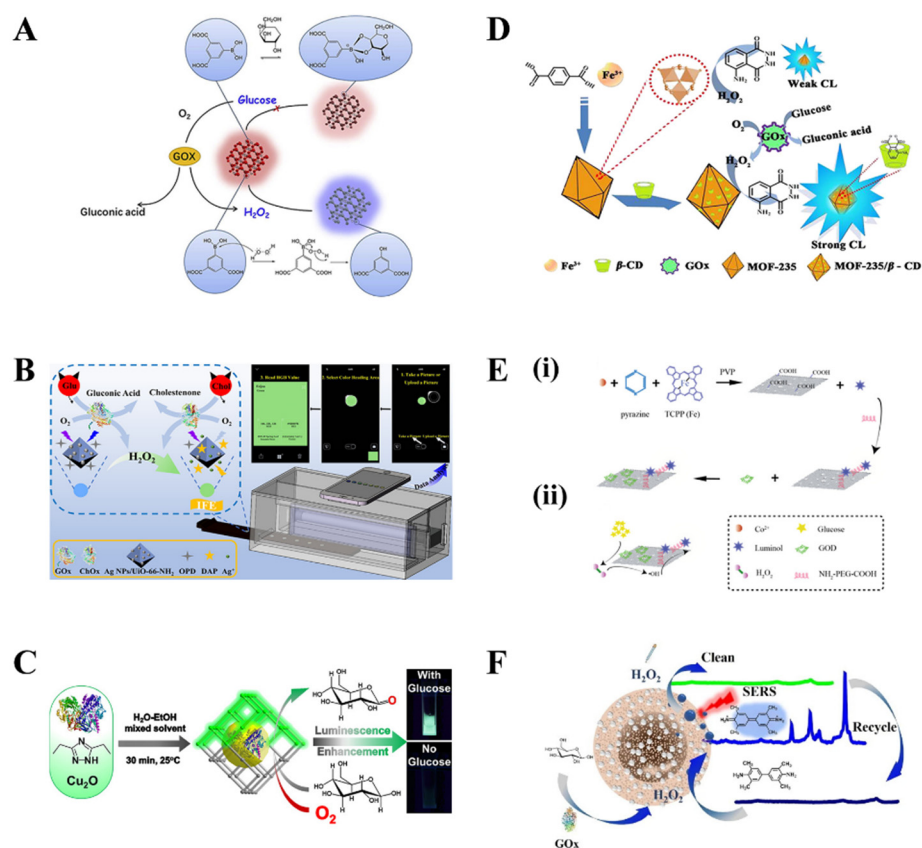


**Figure 8.** (A) Reaction mechanism of FL detection of glucose based on an Eu-MOF (reproduced with permission from [157], copyright © 2019, Elsevier). (B) The smartphone-based Ag NPs/Uio-66-NH<sub>2</sub> and OPD composite film for glucose detection (reproduced with permission from [160], copyright © 2021, American Chemical Society). (C) Synthesis of the GOx@MAF-2 composite and its application in glucose detection (reproduced with permission from [23], copyright © 2019, John Wiley and Sons). (D) CL enhancement mechanism of the luminol-H<sub>2</sub>O<sub>2</sub> system by MOF-235/ $\beta$ -CD composite (reproduced with permission from [23], copyright © 2018, Elsevier). (E) Principle of the novel CL sensor for one-step ultrasensitive glucose detection (i) preparation of Co-TCPP(Fe)@luminol@GOD; (ii) process of one-step detection for glucose (reproduced with permission from [90], copyright © 2019, American Chemical Society). (F) Fabrication and detection principle of MMA (reproduced with permission from [159], copyright © 2022, Springer Nature).

Yang et al. modified AuNPs on the 2D metalloporphyrinic MOF (Cu-tetra(4-carboxyphenyl) porphyrin chloride(Fe(III)), Cu-TCPP(Fe)) in situ, named Au NPs/Cu-TCPP(Fe) [75]. Au NPs converted glucose in saliva to H<sub>2</sub>O<sub>2</sub>, and then H<sub>2</sub>O<sub>2</sub> can be catalyzed by Cu-TCPP(Fe) nanosheets to oxidize leucomalachite green (LMG) into the malachite green (MG), which is a Raman-active molecule. Subsequently, the detection of MG could be performed using SERS. SERS activity is also enhanced in the presence of Au NPs. The linear range of glucose detection is 0.16–8 mM, and the LOD is 3.9  $\mu$ M ( $S/N = 3$ ) without interference from fructose, lactose, and maltose in saliva.

Cui et al. developed a highly sensitive SERS probe named MBs@MIL-100(Fe)@Ag(MMA) (Figure 8F) [159]. This probe demonstrated excellent SERS activity and peroxidase-like catalytic activity, making it ideal for glucose detection. The probe utilized the catalytic cascade reaction between MMA and GOx using TMB molecules enriched by MMA as Raman beacons, resulting in remarkable sensitivity in detecting glucose. Based on the enrichment and size screening capabilities of MIL-100(Fe), MMA has excellent anti-interference properties, allowing it to specifically enrich indicator molecules even in non-ferrous beverages or complex biological fluids (saliva) while excluding the influence of other impurities (dyes, proteins, etc.). In addition, the self-cleaning properties of MMA permitted the recycling of

the probe for detection, which reduced the cost of the solution and provided a new versatile strategy for the accurate detection of glucose in complex samples such as biofluids and food and beverages.

The preparation process of MOF-based SERS substrates is simpler than the conventional SERS substrate preparation process. However, the SERS-enhanced mechanism of MOF-based substrates is still unclear. Further research is needed regarding practicality, portability, and commercialization.

## 4. Novel MOF-Based Glucose Detection Devices

### 4.1. Flexible Wearable Devices for Glucose Detection

Compared to traditional glucose sensors, flexible wearable devices have emerged as highly promising tools for in situ biomarker analysis in body fluids, such as sweat and interstitial fluids, providing a means to monitor blood glucose levels [169]. Sweat glucose has shown a qualitative correlation with blood glucose levels [170], and the integration of flexible electrodes with printed circuit boards (PCBs) has enabled the development of complete wearable devices. When coupled with mobile devices using wireless communication technology, these wearables allow for real-time data collection, transmission, and analysis [171]. It has been reported that there are about 450 million cases of diabetes worldwide, and the number may reach 700 million by 2045 [172]. Compared to traditional glucose testers, flexible wearable glucose-sensing devices offer the advantages of portability, comfort, and real-time monitoring, making them highly desirable for the growing number of diabetes cases worldwide [163].

Hu et al. developed a highly stretchable wearable electrochemical sensor called NCGP fiber for tracking glucose levels in sweat [140]. The sensor was based on a Ni-Co metal-organic framework/Ag/reduced graphene oxide/polyurethane (Ni-Co MOF/Ag/rGO/PU) composite, which was prepared using an improved wet spinning technique. The Ni-Co MOF nanosheets were coated onto the surface of reduced graphene oxide/polyurethane fiber (rGO/PU), along with conductive Ag glue (Figure 9A). This NCGP fiber sensor exhibited excellent electrocatalytic performance for glucose detection, with a linear range from 10  $\mu\text{M}$  to 0.66 mM, a sensitivity of 425.9  $\mu\text{A mM}^{-1} \text{cm}^{-2}$ , and a low limit of detection (LOD) of 3.28  $\mu\text{M}$  ( $S/N = 3$ ). Similarly, Liu et al. successfully manufactured a MOF film using a “coffee ring”-inspired approach, creating a hierarchical and oriented pore structure for improved electron transport efficiency (Figure 9B) [148]. The resulting MOF film-based sweat sensor demonstrated a linear range from 5  $\mu\text{M}$  to 1775  $\mu\text{M}$ , a sensitivity of 1.69 mA  $\text{mM}^{-1} \text{cm}^{-2}$ , and a LOD of 2  $\mu\text{M}$  ( $S/N = 3$ ). These innovative approaches offer promising solutions for non-invasive glucose monitoring, showcasing the potential of MOF-based materials in wearable sensing devices.

Wu et al. developed a multi-enzyme system by immobilizing highly loaded enzymes in a nanocage-based zeolite imidazole framework (NC-ZIF) using a dual restriction strategy to obtain GOx/Hemin@NC-ZIF [24]. The enzyme protection has two lines of defense, the outer shell of NC-ZIF and the inner nanocage of NC-ZIF. In addition to preventing enzyme leakage, the commodious internal space refrains from disrupting enzyme primitive conformation. The resulting GOx/Hemin@NC-ZIF multi-enzyme system exhibits 8.3- and 16-fold higher catalytic cascade activity than free enzymes in a solution in colorimetric and electrochemical sensors for glucose detection, and it also demonstrates long-term stability, excellent selectivity, and reusability (Figure 9C). At an applied potential of 0.6 V, the system showed a good linear range of 50–600  $\mu\text{M}$  and a LOD of 2  $\mu\text{M}$  ( $S/N = 3$ ). Continuous glucose monitoring of sweat was successfully achieved by integrating an enzyme@NC-ZIF-based sensor and PCB into the sweatband and connecting it to a smartphone via Bluetooth.

In addition to detecting glucose in sweat, a MOF-based mouthguard sensor can also be developed to detect glucose in saliva. Moreover, MOFs and their carbon derivatives possess excellent electron-capture capacities and multifunctional structures, making them ideal as active electrode materials for triboelectric nanogenerators (TENG) [173]. By incorporating MOF-based TENG into the design of flexible wearable devices, the potential of self-powered,

environmentally friendly, and powerful wearable glucose-monitoring devices becomes promising [174]. Another avenue for improvement lies in refining the wearable device from the software side. By combining flexible wearable devices with deep learning algorithms, meaningful information can be extracted from the collected data to predict subsequent blood glucose levels with greater accuracy and efficiency [175,176].

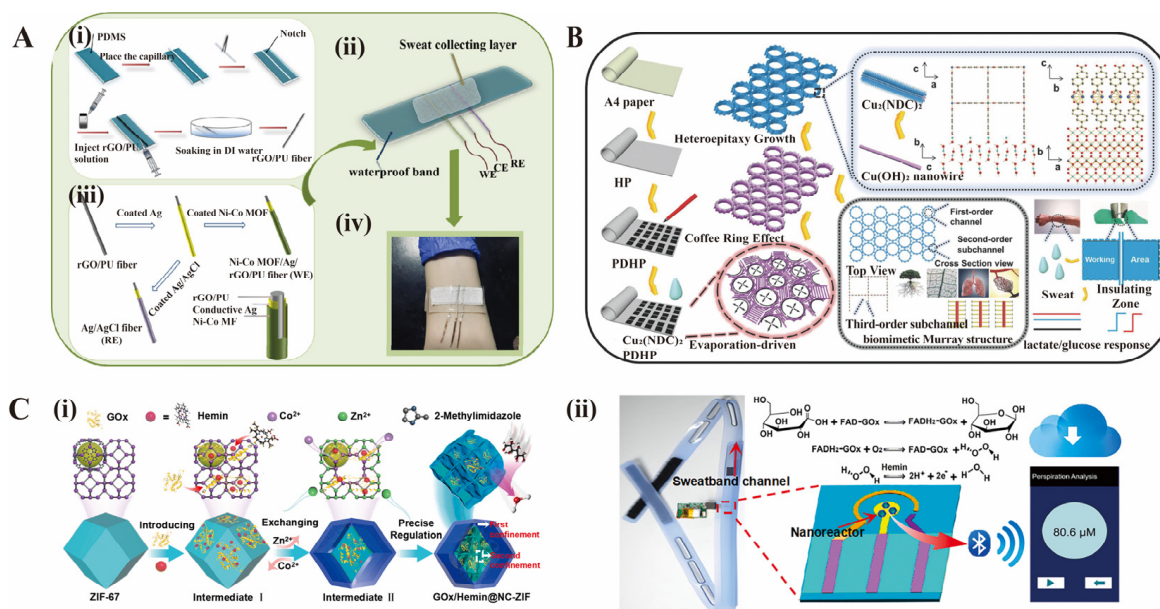


**Figure 9.** (A) Schematic illustration of (i) production of rGO/PU fiber, (ii) manufacturing process of the NCGP working electrode and Ag/AgCl fiber reference electrode, (iii) the NCGP glucose sensor integrated into the elastic fabric, and (iv) the physical image of the device attached to the volunteer's arm (reproduced with permission from [140], copyright © 2021, American Chemical Society). (B) The fabrication process of biomimetic Murray  $\text{Cu}_2(\text{NDC})_2/\text{PDHP}$  (reproduced with permission from [148], copyright © 2018, John Wiley and Sons). (C) (i) Schematic illustration of the synthetic route of  $\text{GOx}/\text{Hemin}@/\text{NC-ZIF}$ ; (ii) Left: A photograph of a sweatband integrated with the portable prototype glucose sensor. Middle: Scheme of the  $\text{GOx}/\text{Hemin}@/\text{NC-ZIF}$  catalytic cascade reaction based on the electrochemical biosensor and the all-integrated sensor fabricated on a polyimide (PI) sheet. Right: A photograph of the smartphone with an app for the perspiration analysis (reproduced with permission from [24], copyright © 2022, Elsevier).

#### 4.2. Microfluidic Chips for Glucose Detection

The miniaturized total analytical system ( $\mu\text{TAS}$ ), sometimes called lab-on-chip (LOC), integrates the operations of chemistry and/or biology experiments (e.g., sample handling, separation, reaction, testing, etc.) on a small chip for fast and accurate analyses of a handful of samples [177]. The first microfluidic paper-based analytical device ( $\mu\text{PAD}$ ) was proposed by Whitesides et al. in 2007, and since then,  $\mu\text{PADs}$  have become one of the most popular POCT platforms [178]. A  $\mu\text{PAD}$  is typically made of paper with a liquid channel and a reaction zone that allows a sample to be injected into the paper and moved to the reaction zone for analysis through capillary force and absorption by the paper fibers. Moreover, it is cost-effective and easy to read [179]. In the POCT process, the analyte is sensed by the functionalized paper, and then the color signal is reported [163]. Gomez et al. utilized Fe-centered porphyrinic Zr-PCN-222(Fe) MOF for encapsulating  $\text{GOx}$  to make well-based and lateral-flow assay (LFA)-based  $\mu\text{PADs}$  [162]. Employing the peroxidase-like activity of Zr-PCN-222(Fe), MOF can achieve colorimetric detection of glucose on these purpose-made  $\mu\text{PADs}$  (Figure 10A,B). The well-based  $\mu\text{PAD}$ , where reaction, mixing, and analysis are all conducted in a single "well", prevents sample loss and has a lower detection limit compared to the LFA-based  $\mu\text{PAD}$ . However, well-based and LFA-based

$\mu$ PADs take too long to detect glucose, 3.5 and 2 h, respectively, and there is subjective uncertainty in the assessment of color by the naked eye. As traditional spectrometers struggle to identify paper colors, many people tend to use mobile apps. Al Lawati et al. designed a disposable 3D  $\mu$ PAD that can use a smartphone to record the color of a paper chip after sample injection within 3–40 min (Figure 10C) [25]. The  $\text{CeO}_2$  NPs@ $\text{NH}_2$ -MIL-88B(Fe)/TMB/specific enzyme complex was loaded in each detection zone. Simultaneous quantification of glucose, fructose, sucrose, and maltose in food and biological samples was successfully achieved by using a distribution layer to disperse samples from the sample injection layer to the four detection zones of the detection layer.

Thin, soft, skin-compatible microfluidic systems have rocketed to popularity in recent years, which are composed of inlet/outlet ports, microfluidic channels, microreservoirs, and colorimetric sensors to collect, capture, store, and analyze sweat [180]. Apart from the paper base, combining skin-interfaced microfluidic systems with MOF-based colorimetric devices may also be a good solution for glucose detection.

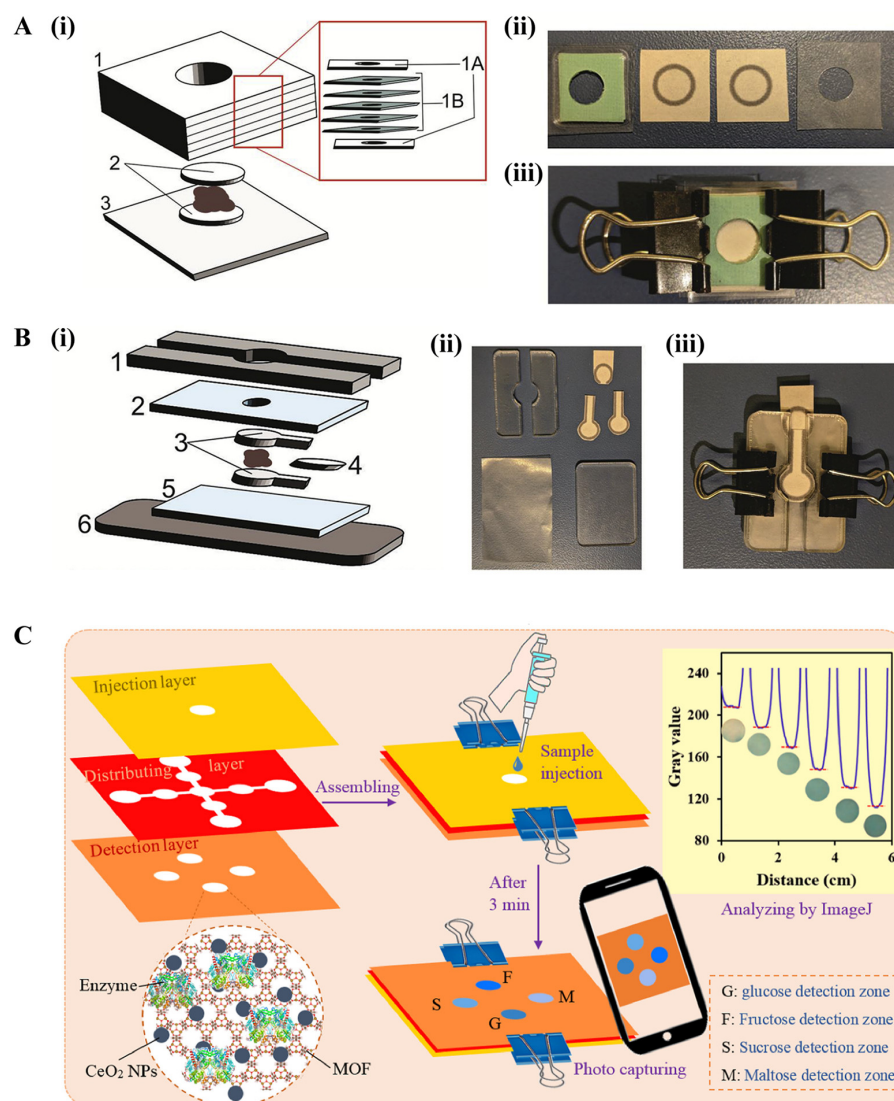


**Figure 10.** (A) (i) Schematic of the well-based  $\mu$ PAD; (ii) well-based  $\mu$ PAD layers; and (iii) assembled chip. (B) (i) Schematic of LFA-based  $\mu$ PAD; (ii) layers; and (iii) assembled chip (reproduced with permission from [162], copyright © 2019, Elsevier). (C) Schematic design for the simultaneous determination of different sugars using a  $\text{CeO}_2$ @ $\text{NH}_2$ -MIL-88B(Fe)-modified paper-based analytical device (reproduced with permission from [25], copyright © 2022, Elsevier).

## 5. Conclusions

In this review, we summarized the various preparation strategies for four types of MOF-based materials utilized in glucose detection: pristine MOFs, nano-particles in/on MOFs, enzymes in/on MOFs, and MOF-derived materials. We have also explored the two primary mechanisms for MOF-based glucose sensors: electrochemical and optical methods. Notably, this review highlights the significant advancements in flexible wearable sensors and microfluidic chips for glucose sensing. The exceptional properties of MOF materials, such as their large specific surface area, tunable pores, abundant active sites, and diverse capabilities (including catalysis and fluorescence), play crucial roles in the development of glucose sensors. For instance, for electrochemical-based glucose sensors, the large specific surface area of MOFs aids in the immobilization of GOx or promotes the conductivity of modified electrodes. On the other hand, optical-based glucose sensors benefit from the enzyme-like activities or fluorescence properties of MOFs, enabling a more visualized and convenient glucose-detection process. As we move forward, the potential of MOF-based electrochemical flexible wearable devices, such as sweatbands and mouthguards, along with optical skin-like biosensors and skin-compatible microfluidic systems, appears highly promising for the future of glucose and other biological analyte detection.

**Author Contributions:** Conceptualization, Y.Z., Q.L., S.-Y.L. and Z.D.; writing—original draft preparation, Y.Z. and Q.L.; writing—review and editing, Y.S., S.-Y.L. and Z.D.; visualization, J.H., M.C. and R.O.; funding acquisition, S.-Y.L. and Z.D. All authors have read and agreed to the published version of the manuscript.

**Funding:** This research was funded by the National Natural Science Foundations of China (22274169), the Scientific Technology Project of Shenzhen City (JCYJ20210324120601004), the Guangdong Natural Science Foundation (2022A1515011318), and the Guangdong Science and Technology Plan Project Grant (2020B1212060077).

**Data Availability Statement:** No new data were created or analyzed in this study. Data sharing is not applicable to this article.

**Conflicts of Interest:** The authors declare no conflict of interest.

## References

1. Pliszka, M.; Szab lewski, L. Glucose transporters as a target for anticancer therapy. *Cancers* **2021**, *13*, 4184. [[CrossRef](#)]
2. Wang, K.; Wu, C.; Wang, F.; Jing, N.; Jiang, G. Co/Co<sub>3</sub>O<sub>4</sub> Nanoparticles Coupled with Hollow Nanoporous Carbon Polyhedrons for the Enhanced Electrochemical Sensing of Acetaminophen. *ACS Sustain. Chem. Eng.* **2019**, *7*, 18582–18592. [[CrossRef](#)]
3. American Diabetes Association. 10. Cardiovascular disease and risk management: Standards of medical care in diabetes—2021. *Diabetes Care* **2020**, *44*, S125–S150.
4. Resmini, E.; Minuto, F.; Colao, A.; Ferone, D. Secondary diabetes associated with principal endocrinopathies: The impact of new treatment modalities. *Acta Diabetol.* **2009**, *46*, 85–95. [[CrossRef](#)] [[PubMed](#)]
5. American Diabetes Association. 6. Glycemic targets: Standards of medical care in diabetes-2021. *Diabetes Care* **2021**, *44*, S73–S84. [[CrossRef](#)] [[PubMed](#)]
6. Do, H.H.; Cho, J.H.; Han, S.M.; Ahn, S.H.; Kim, S.Y. Metal-organic-framework- and mxene-based taste sensors and glucose detection. *Sensors* **2021**, *21*, 7423. [[CrossRef](#)] [[PubMed](#)]
7. Mohamad Nor, N.; Ridhuan, N.S.; Abdul Razak, K. Progress of enzymatic and non-enzymatic electrochemical glucose biosensor based on nanomaterial-modified electrode. *Biosensors* **2022**, *12*, 1136. [[CrossRef](#)]
8. van Enter, B.J.; von Hauff, E. Challenges and perspectives in continuous glucose monitoring. *Chem. Commun.* **2018**, *54*, 5032–5045. [[CrossRef](#)]
9. Galant, A.L.; Kaufman, R.C.; Wilson, J.D. Glucose: Detection and analysis. *Food Chem.* **2015**, *188*, 149–160. [[CrossRef](#)]
10. Gao, Q.; Bai, Q.; Zheng, C.; Sun, N.; Liu, J.; Chen, W.; Hu, F.; Lu, T. Application of metal-organic framework in diagnosis and treatment of diabetes. *Biomolecules* **2022**, *12*, 1240. [[CrossRef](#)]
11. Adeel, M.; Asif, K.; Rahman, M.M.; Daniele, S.; Canzonieri, V.; Rizzolio, F. Glucose detection devices and methods based on metal-organic frameworks and related materials. *Adv. Funct. Mater.* **2021**, *31*, 2106023. [[CrossRef](#)]
12. Tian, L.; Huang, Z.; Lu, X.; Wang, T.; Cheng, W.; Yang, H.; Huang, T.; Li, T.; Li, Z. Plasmon-mediated oxidase-like activity on Ag@ZnS heterostructured hollow nanowires for rapid visual detection of nitrite. *Inorg. Chem.* **2023**, *62*, 1659–1666. [[CrossRef](#)] [[PubMed](#)]
13. Shang, H.; Zhang, X.; Ding, M.; Zhang, A.; Wang, C. A smartphone-assisted colorimetric and photothermal probe for glutathione detection based on enhanced oxidase-mimic CoFeCe three-atom nanozyme in food. *Food Chem.* **2023**, *423*, 136296. [[CrossRef](#)]

14. Wang, N.; Zhang, L.; Li, Z.; Zhou, C.; Lv, Y.; Su, X. A sensing platform for on-site detection of glutathione S-transferase using oxidized Pi@Ce-doped Zr-based metal-organic frameworks(MOFs). *Talanta* **2023**, *259*, 124537. [[CrossRef](#)]
15. Cheng, S.; Gao, X.; Delacruz, S.; Chen, C.; Tang, Z.; Shi, T.; Carraro, C.; Maboudian, R. In situ formation of metal-organic framework derived CuO polyhedrons on carbon cloth for highly sensitive non-enzymatic glucose sensing. *J. Mater. Chem. B* **2019**, *7*, 4990–4996. [[CrossRef](#)]
16. Li, X.; Dong, H.; Fan, Q.; Chen, K.; Sun, D.; Hu, T.; Ni, Z. One-pot, rapid microwave-assisted synthesis of bimetallic metal-organic framework for efficient enzyme-free glucose detection. *Microchem. J.* **2022**, *179*, 107468. [[CrossRef](#)]
17. Meng, W.; Wen, Y.; Dai, L.; He, Z.; Wang, L. A novel electrochemical sensor for glucose detection based on Ag@ZIF-67 nanocomposite. *Sens. Actuators B Chem.* **2018**, *260*, 852–860.
18. Li, J.; Zhao, J.; Li, S.; Chen, Y.; Lv, W.; Zhang, J.; Zhang, L.; Zhang, Z.; Lu, X. Synergistic effect enhances the peroxidase-like activity in platinum nanoparticle-supported metal-organic framework hybrid nanozymes for ultrasensitive detection of glucose. *Nano Res.* **2021**, *14*, 4689–4695. [[CrossRef](#)]
19. Lin, Q.; Huang, J.; Zhang, Y.; Chen, M.; Xu, Y.; Zou, X.; Liu, S.-Y.; Dai, Z. A smartphone-assisted “all-in-one” paper chip for one-pot noninvasive detection of salivary glucose level. *Chem. Eng. J.* **2023**, *468*, 143608. [[CrossRef](#)]
20. Ma, X.; Tang, K.-L.; Yang, M.; Shi, W.; Zhao, W. Metal-organic framework-derived yolk-shell hollow Ni/NiO@C microspheres for bifunctional non-enzymatic glucose and hydrogen peroxide biosensors. *J. Mater. Sci.* **2021**, *56*, 442–456. [[CrossRef](#)]
21. Sun, Q.; Ding, J.; Chen, D.; Han, C.; Jiang, M.; Li, T.-T.; Hu, Y.; Qian, J.; Huang, S. Silica-Templated Metal Organic Framework-Derived Hierarchically Porous Cobalt Oxide in Nitrogen-Doped Carbon Nanomaterials for Electrochemical Glucose Sensing. *ChemElectroChem* **2021**, *8*, 812–818. [[CrossRef](#)]
22. Haldorai, Y.; Choe, S.R.; Huh, Y.S.; Han, Y.-K. Metal-organic framework derived nanoporous carbon/Co<sub>3</sub>O<sub>4</sub> composite electrode as a sensing platform for the determination of glucose and high-performance supercapacitor. *Carbon* **2018**, *127*, 366–373. [[CrossRef](#)]
23. Xu, Y.; Liu, S.-Y.; Liu, J.; Zhang, L.; Chen, D.; Chen, J.; Ma, Y.; Zhang, J.-P.; Dai, Z.; Zou, X. In Situ Enzyme Immobilization with Oxygen-Sensitive Luminescent Metal-Organic Frameworks to Realize “All-in-One” Multifunctions. *Chem. Eur. J.* **2019**, *25*, 5463–5471. [[CrossRef](#)] [[PubMed](#)]
24. Wang, Q.; Chen, M.; Xiong, C.; Zhu, X.; Chen, C.; Zhou, F.; Dong, Y.; Wang, Y.; Xu, J.; Li, Y.; et al. Dual confinement of high-loading enzymes within metal-organic frameworks for glucose sensor with enhanced cascade biocatalysis. *Biosens. Bioelectron.* **2022**, *196*, 113695. [[CrossRef](#)] [[PubMed](#)]
25. Hassanzadeh, J.; Al Lawati, H.A.J.; Bagheri, N. On paper synthesis of multifunctional CeO<sub>2</sub> nanoparticles@Fe-MOF composite as a multi-enzyme cascade platform for multiplex colorimetric detection of glucose, fructose, sucrose, and maltose. *Biosens. Bioelectron.* **2022**, *207*, 114184. [[CrossRef](#)]
26. Mao, X.; Lu, Y.; Zhang, X.; Huang, Y. beta-Cyclodextrin functionalization of metal-organic framework MOF-235 with excellent chemiluminescence activity for sensitive glucose biosensing. *Talanta* **2018**, *188*, 161–167. [[CrossRef](#)]
27. Chen, C.; Xiong, D.; Gu, M.; Lu, C.; Yi, F.-Y.; Ma, X. MOF-Derived Bimetallic CoFe-PBA Composites as Highly Selective and Sensitive Electrochemical Sensors for Hydrogen Peroxide and Nonenzymatic Glucose in Human Serum. *ACS Appl. Mater. Interfaces* **2020**, *12*, 35365–35374. [[CrossRef](#)]
28. Wen, Y.; Meng, W.; Li, C.; Dai, L.; He, Z.; Wang, L.; Li, M.; Zhu, J. Enhanced glucose sensing based on a novel composite Co(II)-MOF/Acb modified electrode. *Dalton Trans.* **2018**, *47*, 3872–3879. [[CrossRef](#)] [[PubMed](#)]
29. Ling, W.; Liew, G.; Li, Y.; Hao, Y.; Pan, H.; Wang, H.; Ning, B.; Xu, H.; Huang, X. Materials and Techniques for Implantable Nutrient Sensing Using Flexible Sensors Integrated with Metal-Organic Frameworks. *Adv. Mater.* **2018**, *30*, e1800917. [[CrossRef](#)]
30. Bagheri, N.; Dastborhan, M.; Khataee, A.; Hassanzadeh, J.; Kobya, M. Synthesis of g-C<sub>3</sub>N<sub>4</sub>@CuMOFs nanocomposite with superior peroxidase mimetic activity for the fluorometric measurement of glucose. *Spectrochim. Acta Part A* **2019**, *213*, 28–36. [[CrossRef](#)]
31. Zhang, X.; Xu, Y.; Ye, B. An efficient electrochemical glucose sensor based on porous nickel-based metal organic framework/carbon nanotubes composite (Ni-MOF/CNTs). *J. Alloys Compd.* **2018**, *767*, 651–656. [[CrossRef](#)]
32. Li, W.; Lv, S.; Wang, Y.; Zhang, L.; Cui, X. Nanoporous gold induced vertically standing 2D NiCo bimetal-organic framework nanosheets for non-enzymatic glucose biosensing. *Sens. Actuators B Chem.* **2019**, *281*, 652–658. [[CrossRef](#)]
33. Rezki, M.; Septiani, N.L.W.; Iqbal, M.; Adhika, D.R.; Wenten, I.G.; Yulianto, B. Review—Recent advance in multi-metallic metal organic frameworks (MM-MOFs) and their derivatives for electrochemical biosensor application. *J. Electrochem. Soc.* **2022**, *169*, 017504. [[CrossRef](#)]
34. Song, S.; Ma, X.; Li, W.; Zhang, B.; Shao, B.; Chang, X.; Liu, X. Novel stylophora coral-like furan-based Ni/Co bimetallic metal organic framework for high-performance capacitive storage and non-enzymatic glucose electrochemical sensing. *J. Alloys Compd.* **2023**, *931*, 167413. [[CrossRef](#)]
35. Stock, N.; Biswas, S. Synthesis of metal-organic frameworks (MOFs): Routes to various mof topologies, morphologies, and composites. *Chem. Rev.* **2012**, *112*, 933–969. [[CrossRef](#)]
36. Demazeau, G. Solvothermal processes: Definition, key factors governing the involved chemical reactions and new trends. *Z. Für Naturforschung B* **2010**, *65*, 999–1006. [[CrossRef](#)]
37. Ghosh, A.; Fathima, T.K.S.; Ramaprabhu, S. Effect of Coordinated Solvent Molecules in Cu-MOF on Enzyme Free Sensing of Glucose and Lactate in Physiological pH. *J. Electrochem. Soc.* **2022**, *169*, 057524. [[CrossRef](#)]

38. Demazeau, G.; Largeteau, A. Hydrothermal/solvothermal crystal growth: An old but adaptable process. *Z. Anorg. Allg. Chem.* **2015**, *641*, 159–163. [[CrossRef](#)]
39. Zha, X.; Yang, W.; Shi, L.; Li, Y.; Zeng, Q.; Xu, J.; Yang, Y. Morphology control strategy of bimetallic mof nanosheets for upgrading the sensitivity of noninvasive glucose detection. *ACS Appl. Mater. Interfaces* **2022**, *14*, 37843–37852. [[CrossRef](#)]
40. Du, Q.; Liao, Y.; Shi, N.; Sun, S.; Liao, X.; Yin, G.; Huang, Z.; Pu, X.; Wang, J. Facile synthesis of bimetallic metal-organic frameworks on nickel foam for a high performance non-enzymatic glucose sensor. *J. Electroanal. Chem.* **2022**, *904*, 115887. [[CrossRef](#)]
41. Yuan, A.; Lu, Y.; Zhang, X.; Chen, Q.; Huang, Y. Two-dimensional iron MOF nanosheet as a highly efficient nanozyme for glucose biosensing. *J. Mater. Chem. B* **2020**, *8*, 9295–9303. [[CrossRef](#)]
42. Arul, P.; Gowthaman, N.S.K.; John, S.A.; Tominaga, M. Tunable electrochemical synthesis of 3D nucleated microparticles like Cu-BTC MOF-carbon nanotubes composite: Enzyme free ultrasensitive determination of glucose in a complex biological fluid. *Electrochim. Acta* **2020**, *354*, 136673. [[CrossRef](#)]
43. Ma, Z.-Z.; Ma, Y.; Liu, B.; Xu, L.; Jiao, H. A high-performance Co-MOF non-enzymatic electrochemical sensor for glucose detection. *New J. Chem.* **2021**, *45*, 21350–21358. [[CrossRef](#)]
44. Abrori, S.A.; Trisno, M.L.A.; Aritonang, R.A.; Anshori, I.; Nugraha; Suyatman; Yulianto, B. Synthesis and characterization of metal-organic framework (MOF) CoBTC as a non-enzymatic electrochemical biosensor for glucose. *IOP Conf. Ser. Mater. Sci. Eng.* **2021**, *1045*, 012006. [[CrossRef](#)]
45. Pan, W.; Zheng, Z.; Wu, X.; Gao, J.; Liu, Y.; Yuan, Q.; Gan, W. Facile synthesis of 2D/3D hierarchical NiCu bimetallic MOF for non-enzymatic glucose sensor. *Microchem. J.* **2021**, *170*, 106652. [[CrossRef](#)]
46. Xu, Z.; Wang, Q.; Hui, Z.; Zhao, S.; Zhao, Y.; Wang, L. Carbon cloth-supported nanorod-like conductive Ni/Co bimetal MOF: A stable and high-performance enzyme-free electrochemical sensor for determination of glucose in serum and beverage. *Food Chem.* **2021**, *349*, 129202.
47. Liu, Q.; Chen, J.; Yu, F.; Wu, J.; Liu, Z.; Peng, B. Multifunctional book-like CuCo-MOF for highly sensitive glucose detection and electrocatalytic oxygen evolution. *New J. Chem.* **2021**, *45*, 16714–16721. [[CrossRef](#)]
48. Bagheri, A.R.; Aramesh, N. Towards the room-temperature synthesis of covalent organic frameworks: A mini-review. *J. Mater. Sci.* **2021**, *56*, 1116–1132. [[CrossRef](#)]
49. Wei, Z.; Zhu, W.; Li, Y.; Ma, Y.; Wang, J.; Hu, N.; Suo, Y.; Wang, J. Conductive leaflike cobalt metal-organic framework nanoarray on carbon cloth as a flexible and versatile anode toward both electrocatalytic glucose and water oxidation. *Inorg. Chem.* **2018**, *57*, 8422–8428. [[CrossRef](#)]
50. Li, P.; Bai, Y.; Zhang, G.; Guo, X.; Meng, X.; Pang, H. Surface-halogen-introduced 2D NiCo bimetallic MOFs via a modulation method for elevated electrochemical glucose sensing. *Inorg. Chem. Front.* **2022**, *9*, 5853–5861. [[CrossRef](#)]
51. Song, D.; Wang, L.; Qu, Y.; Wang, B.; Li, Y.; Miao, X.; Yang, Y.; Duan, C. A High-Performance Three-Dimensional Hierarchical Structure MOF-Derived NiCo LDH Nanosheets for Non-Enzymatic Glucose Detection. *J. Electrochem. Soc.* **2019**, *166*, B1681–B1688. [[CrossRef](#)]
52. Lin, C.; Du, Y.; Wang, S.; Wang, L.; Song, Y. Glucose oxidase@Cu-hemin metal-organic framework for colorimetric analysis of glucose. *Mater. Sci. Eng. C* **2021**, *118*, 111511. [[CrossRef](#)] [[PubMed](#)]
53. Chen, C.; Wang, Y.-L.; Lin, X.; Ma, S.-H.; Cao, J.-T.; Liu, Y.-M. Cu-MOFs/GOx Bifunctional Probe-Based Synergistic Signal Amplification Strategy: Toward Highly Sensitive Closed Bipolar Electrochemiluminescence Immunoassay. *ACS Appl. Mater. Interfaces* **2023**, *15*, 22959–22966. [[CrossRef](#)] [[PubMed](#)]
54. Hu, S.; Lin, Y.; Teng, J.; Wong, W.-L.; Qiu, B. In situ deposition of MOF-74(Cu) nanosheet arrays onto carbon cloth to fabricate a sensitive and selective electrocatalytic biosensor and its application for the determination of glucose in human serum. *Microchim. Acta* **2020**, *187*, 670. [[CrossRef](#)] [[PubMed](#)]
55. Zhao, Z.; Kong, Y.; Lin, X.; Liu, C.; Liu, J.; He, Y.; Yang, L.; Huang, G.; Mei, Y. Oxide nanomembrane induced assembly of a functional smart fiber composite with nanoporosity for an ultra-sensitive flexible glucose sensor. *J. Mater. Chem. A* **2020**, *8*, 26119–26129. [[CrossRef](#)]
56. Phan, P.T.; Hong, J.; Tran, N.; Le, T.H. The properties of microwave-assisted synthesis of metal-organic frameworks and their applications. *Nanomaterials* **2023**, *13*, 352. [[CrossRef](#)] [[PubMed](#)]
57. Vaitsis, C.; Sourkouni, G.; Argiris, C. Metal organic frameworks (MOFs) and ultrasound: A review. *Ultrason. Sonochem.* **2019**, *52*, 106–119. [[CrossRef](#)]
58. Zeraati, M.; Alizadeh, V.; Kazemzadeh, P.; Safinejad, M.; Kazemian, H.; Sargazi, G. A new nickel metal organic framework (Ni-MOF) porous nanostructure as a potential novel electrochemical sensor for detecting glucose. *J. Porous Mater.* **2022**, *29*, 257–267. [[CrossRef](#)]
59. Friščič, T. New opportunities for materials synthesis using mechanochemistry. *J. Mater. Chem.* **2010**, *20*, 7599–7605. [[CrossRef](#)]
60. Koyappayil, A.; Yeon, S.-H.; Chavan, S.G.; Jin, L.; Go, A.; Lee, M.-H. Efficient and rapid synthesis of ultrathin nickel-metal organic framework nanosheets for the sensitive determination of glucose. *Microchem. J.* **2022**, *179*, 107462. [[CrossRef](#)]
61. Al-Kutubi, H.; Gascon, J.; Sudhölter, E.J.R.; Rassaei, L. Electrosynthesis of Metal–Organic Frameworks: Challenges and Opportunities. *ChemElectroChem* **2015**, *2*, 462–474. [[CrossRef](#)]

62. de Carvalho, M.H.; de Araújo, H.D.A.; da Silva, R.P.; dos Santos Correia, M.T.; de Freitas, K.C.S.; de Souza, S.R.; Barroso Coelho, L.C.B. Biosensor Characterization from Cratylia mollis Seed Lectin (Cramoll)-MOF and Specific Carbohydrate Interactions in an Electrochemical Model. *Chem. Biodivers.* **2022**, *19*, e202200515. [CrossRef]
63. Shahrokhian, S.; Ezzati, M.; Hosseini, H. Fabrication of a sensitive and fast response electrochemical glucose sensing platform based on co-based metal-organic frameworks obtained from rapid in situ conversion of electrodeposited cobalt hydroxide intermediates. *Talanta* **2020**, *210*, 120696. [CrossRef]
64. Wang, X.; Wang, Y.; Ying, Y. Recent advances in sensing applications of metal nanoparticle/metal-organic framework composites. *TrAC Trends Anal. Chem.* **2021**, *143*, 116395. [CrossRef]
65. Xiang, W.; Zhang, Y.; Lin, H.; Liu, C.-J. Nanoparticle/metal-organic framework composites for catalytic applications: Current status and perspective. *Molecules* **2017**, *22*, 2103. [CrossRef] [PubMed]
66. Zhang, Y.; Wei, X.; Gu, Q.; Zhang, J.; Ding, Y.; Xue, L.; Chen, M.; Wang, J.; Wu, S.; Yang, X.; et al. Cascade amplification based on PEI-functionalized metal-organic framework supported gold nanoparticles/nitrogen-doped graphene quantum dots for amperometric biosensing applications. *Electrochim. Acta* **2022**, *405*, 139803. [CrossRef]
67. Li, Y.; Li, J.-J.; Zhang, Q.; Zhang, J.-Y.; Zhang, N.; Fang, Y.-Z.; Yan, J.; Ke, Q. The multifunctional BODIPY@Eu-MOF nanosheets as bioimaging platform: A ratiometric fluorescent sensor for highly efficient detection of  $F^-$ ,  $H_2O_2$  and glucose. *Sens. Actuators B Chem.* **2022**, *354*, 131140.
68. Liu, Y.; Shi, W.-J.; Lu, Y.-K.; Liu, G.; Hou, L.; Wang, Y.-Y. Nonenzymatic Glucose Sensing and Magnetic Property Based on the Composite Formed by Encapsulating Ag Nanoparticles in Cluster-Based Co-MOF. *Inorg. Chem.* **2019**, *58*, 16743–16751. [CrossRef]
69. Zhang, Y.; Zhou, Y.; Zhao, Y.; Liu, C.-J. Recent progresses in the size and structure control of MOF supported noble metal catalysts. *Catal. Today* **2016**, *263*, 61–68. [CrossRef]
70. Zhai, X.; Cao, Y.; Sun, W.; Cao, S.; Wang, Y.; He, L.; Yao, N.; Zhao, D. Core-shell composite N-doped-Co-MOF@polydopamine decorated with Ag nanoparticles for nonenzymatic glucose sensors. *J. Electroanal. Chem.* **2022**, *918*, 116491. [CrossRef]
71. Xu, T.; Zhang, Y.; Liu, M.; Wang, H.; Ren, J.; Tian, Y.; Liu, X.; Zhou, Y.; Wang, J.; Zhu, W.; et al. In-situ two-step electrodeposition of alpha-CD-rGO/Ni-MOF composite film for superior glucose sensing. *J. Alloys Compd.* **2022**, *923*, 166418. [CrossRef]
72. Jin, X.; Li, G.; Xu, T.; Su, L.; Yan, D.; Zhang, X. Ruthenium-based Conjugated Polymer and Metal-organic Framework Nanocomposites for Glucose Sensing. *Electroanalysis* **2021**, *33*, 1902–1910. [CrossRef]
73. Chen, S.; Liu, D.; Song, N.; Wang, C.; Lu, X. Promoting non-enzymatic electrochemical sensing performance toward glucose by the integration of conducting polypyrrole with metal-organic framework. *Compos. Commun.* **2022**, *30*, 101074. [CrossRef]
74. Arif, D.; Hussain, Z.; Sohail, M.; Liaqat, M.A.; Khan, M.A.; Noor, T. A non-enzymatic electrochemical sensor for glucose detection based on Ag@TiO<sub>2</sub>@metal-organic framework (ZIF-67) nanocomposite. *Front. Chem.* **2020**, *8*, 573510. [CrossRef]
75. Hu, S.; Jiang, Y.; Wu, Y.; Guo, X.; Ying, Y.; Wen, Y.; Yang, H. Enzyme-Free Tandem Reaction Strategy for Surface-Enhanced Raman Scattering Detection of Glucose by Using the Composite of Au Nanoparticles and Porphyrin-Based Metal-Organic Framework. *ACS Appl. Mater. Interfaces* **2020**, *12*, 55324–55330. [CrossRef]
76. Ma, Z.-Z.; Wang, Y.-S.; Liu, B.; Jiao, H.; Xu, L. A Non-Enzymatic Electrochemical Sensor of Cu@Co-MOF Composite for Glucose Detection with High Sensitivity and Selectivity. *Chemosensors* **2022**, *10*, 416. [CrossRef]
77. Duraisamy, S.R.; Liu, W.-L.; Huang, H.-Y.; Lin, C.-H. Immobilization of protein on nanoporous metal-organic framework materials. *Comments Inorg. Chem.* **2015**, *35*, 331–349.
78. Kempahanumakkagari, S.; Kumar, V.; Samaddar, P.; Kumar, P.; Ramakrishnappa, T.; Kim, K.H. Biomolecule-embedded metal-organic frameworks as an innovative sensing platform. *Biotechnol. Adv.* **2018**, *36*, 467–481. [CrossRef]
79. Mu, Z.; Wu, S.; Guo, J.; Zhao, M.; Wang, Y. Dual Mechanism Enhanced Peroxidase-like Activity of Iron-Nickel Bimetal-Organic Framework Nanozyme and Its Application for Biosensing. *ACS Sustain. Chem. Eng.* **2022**, *10*, 2984–2993. [CrossRef]
80. Zhou, Z.; Chao, H.; He, W.; Su, P.; Song, J.; Yang, Y. Boosting the activity of enzymes in metal-organic frameworks by a one-stone-two-bird enzymatic surface functionalization strategy. *Appl. Surf. Sci.* **2022**, *586*, 152815. [CrossRef]
81. Shen, H.; Shi, H.; Yang, Y.; Song, J.; Ding, C.; Yu, S. Highly efficient synergistic biocatalysis driven by stably loaded enzymes within hierarchically porous iron/cobalt metal-organic framework via biomimetic mineralization. *J. Mater. Chem. B* **2022**, *10*, 1553–1560. [CrossRef]
82. Du, Y.; Jia, X.; Zhong, L.; Jiao, Y.; Zhang, Z.; Wang, Z.; Feng, Y.; Bilal, M.; Cui, J.; Jia, S. Metal-organic frameworks with different dimensionalities: An ideal host platform for enzyme@MOF composites. *Coord. Chem. Rev.* **2022**, *454*, 214327. [CrossRef]
83. Li, S.-F.; Chen, Y.; Wang, Y.-S.; Mo, H.-L.; Zang, S.-Q. Integration of enzyme immobilization and biomimetic catalysis in hierarchically porous metal-organic frameworks for multi-enzymatic cascade reactions. *Sci. China Chem.* **2022**, *65*, 1122–1128. [CrossRef]
84. Goud, B.S.; Shin, G.; Vattikuti, S.V.P.; Mameda, N.; Kim, H.; Koyyada, G.; Kim, J.H. Enzyme-integrated biomimetic cobalt metal-organic framework nanozyme for one-step cascade glucose biosensing via tandem catalysis. *Biochem. Eng. J.* **2022**, *188*, 108669. [CrossRef]
85. Nadar, S.S.; Vaidya, L.; Rathod, V.K. Enzyme embedded metal organic framework (enzyme-MOF): De novo approaches for immobilization. *Int. J. Biol. Macromol.* **2020**, *149*, 861–876. [CrossRef] [PubMed]
86. Chen, T.; Zhang, A.; Cheng, Y.; Zhang, Y.; Fu, D.; Liu, M.; Li, A.; Liu, J. A molecularly imprinted nanoreactor with spatially confined effect fabricated with nano-caged cascaded enzymatic system for specific detection of monosaccharides. *Biosens. Bioelectron.* **2021**, *188*, 113355. [CrossRef]

87. Wang, B.; Luo, Y.; Gao, L.; Liu, B.; Duan, G. High-performance field-effect transistor glucose biosensors based on bimetallic Ni/Cu metal-organic frameworks. *Biosens. Bioelectron.* **2021**, *171*, 112736. [[CrossRef](#)]
88. Zhao, Z.; Huang, Y.; Liu, W.; Ye, F.; Zhao, S. Immobilized glucose oxidase on boronic acid-functionalized hierarchically porous MOF as an integrated nanozyme for one-step glucose detection. *ACS Sustain. Chem. Eng.* **2020**, *8*, 4481–4488. [[CrossRef](#)]
89. Xu, W.; Jiao, L.; Yan, H.; Wu, Y.; Chen, L.; Gu, W.; Du, D.; Lin, Y.; Zhu, C. Glucose oxidase-integrated metal-organic framework hybrids as biomimetic cascade nanozymes for ultrasensitive glucose biosensing. *ACS Appl. Mater. Interfaces* **2019**, *11*, 22096–22101. [[CrossRef](#)]
90. Zhu, N.; Gu, L.; Wang, J.; Li, X.; Liang, G.; Zhou, J.; Zhang, Z. Novel and Sensitive Chemiluminescence Sensors Based on 2D-MOF Nanosheets for One-Step Detection of Glucose in Human Urine. *J. Phys. Chem. C* **2019**, *123*, 9388–9393. [[CrossRef](#)]
91. Zhong, N.; Gao, R.; Shen, Y.; Kou, X.; Wu, J.; Huang, S.; Chen, G.; Ouyang, G. Enzymes-Encapsulated Defective Metal-Organic Framework Hydrogel Coupling with a Smartphone for a Portable Glucose Biosensor. *Anal. Chem.* **2022**, *94*, 14385–14393. [[CrossRef](#)] [[PubMed](#)]
92. Zhang, S.; Zhao, W.; Zeng, J.; He, Z.; Wang, X.; Zhu, Z.; Hu, R.; Liu, C.; Wang, Q. Wearable non-invasive glucose sensors based on metallic nanomaterials. *Mater. Today Bio* **2023**, *20*, 100638. [[CrossRef](#)] [[PubMed](#)]
93. Chen, J.; Ma, Q.; Li, M.; Chao, D.; Huang, L.; Wu, W.; Fang, Y.; Dong, S. Glucose-oxidase like catalytic mechanism of noble metal nanozymes. *Nat. Commun.* **2021**, *12*, 3375. [[CrossRef](#)]
94. Yogesh, M.C.; Satish, B.J.; Padamaja, N.P.; Vikas, V.M.; Jayavant, L.G.; Chandrakant, D.L. Metal oxide-based composites in nonenzymatic electrochemical glucose sensors. *Ind. Eng. Chem. Res.* **2021**, *60*, 18195–18217.
95. Gonçalves, J.M.; Martins, P.R.; Rocha, D.P.; Matias, T.A.; Julião, M.S.S.; Munoz, R.A.A.; Angnes, L. Recent trends and perspectives in electrochemical sensors based on MOF-derived materials. *J. Mater. Chem. C* **2021**, *9*, 8718–8745. [[CrossRef](#)]
96. Lu, X.F.; Fang, Y.; Luan, D.; Lou, X.W.D. Metal-organic frameworks derived functional materials for electrochemical energy storage and conversion: A mini review. *Nano Lett.* **2021**, *21*, 1555–1565. [[CrossRef](#)] [[PubMed](#)]
97. Xiao, W.; Cheng, M.; Liu, Y.; Wang, J.; Zhang, G.; Wei, Z.; Li, L.; Du, L.; Wang, G.; Liu, H. Functional metal/carbon composites derived from metal-organic frameworks: Insight into structures, properties, performances, and mechanisms. *ACS Catal.* **2023**, *13*, 1759–1790. [[CrossRef](#)]
98. Zhao, C.; Tang, X.; Zhao, J.; Cao, J.; Jiang, Z.; Qin, J. MOF derived core-shell CuO/C with temperature-controlled oxygen-vacancy for real time analysis of glucose. *J. Nanobiotechnol.* **2022**, *20*, 507. [[CrossRef](#)] [[PubMed](#)]
99. Zhang, X.; Zhang, Y.; Guo, W.; Wan, K.; Zhang, T.; Arbiol, J.; Zhao, Y.-Q.; Xu, C.-L.; Xu, M.; Fransaer, J. A yolk-albumen-shell structure of mixed Ni-Co oxide with an ultrathin carbon shell for high-sensitivity glucose sensors. *Mater. Adv.* **2020**, *1*, 908–917. [[CrossRef](#)]
100. Archana, V.; Xia, Y.; Fang, R.; Kumar, G.G. Hierarchical CuO/NiO-Carbon Nanocomposite Derived from Metal Organic Framework on Cello Tape for the Flexible and High Performance Nonenzymatic Electrochemical Glucose Sensors. *ACS Sustain. Chem. Eng.* **2019**, *7*, 6707–6719. [[CrossRef](#)]
101. Li, L.; Liu, Y.; Ai, L.; Jiang, J. Synthesis of the crystalline porous copper oxide architectures derived from metal-organic framework for electrocatalytic oxidation and sensitive detection of glucose. *J. Ind. Eng. Chem.* **2019**, *70*, 330–337. [[CrossRef](#)]
102. Chu, D.; Li, F.; Song, X.; Ma, H.; Tan, L.; Pang, H.; Wang, X.; Guo, D.; Xiao, B. A novel dual-tasking hollow cube NiFe<sub>2</sub>O<sub>4</sub>-NiCo-LDH@rGO hierarchical material for high performance supercapacitor and glucose sensor. *J. Colloid Interface Sci.* **2020**, *568*, 130–138. [[CrossRef](#)]
103. Xiao, L.; Yang, K.; Duan, J.; Zheng, S.; Jiang, J. The nickel phosphate rods derived from Ni-MOF with enhanced electrochemical activity for non-enzymatic glucose sensing. *Talanta* **2022**, *247*, 123587. [[CrossRef](#)]
104. Zhu, Q.; Hu, S.; Zhang, L.; Li, Y.; Carraro, C.; Maboudian, R.; Wei, W.; Liu, A.; Zhang, Y.; Liu, S. Reconstructing hydrophobic ZIF-8 crystal into hydrophilic hierarchically-porous nanoflowers as catalyst carrier for nonenzymatic glucose sensing. *Sens. Actuators B Chem.* **2020**, *313*, 128031. [[CrossRef](#)]
105. Zhang, Y.; Huang, Y.; Gao, P.; Yin, W.; Yin, M.; Pu, H.; Sun, Q.; Liang, X.; Fa, H.-b. Bimetal-organic frameworks MnCo-MOF-74 derived Co/MnO@HC for the construction of a novel enzyme-free glucose sensor. *Microchem. J.* **2022**, *175*, 107097. [[CrossRef](#)]
106. Vignesh, A.; Vajeeston, P.; Pannipara, M.; Al-Sehemi, A.G.; Xia, Y.; Kumar, G.G. Bimetallic metal-organic framework derived 3D hierarchical NiO/Co<sub>3</sub>O<sub>4</sub>/C hollow microspheres on biodegradable garbage bag for sensitive, selective, and flexible enzyme-free electrochemical glucose detection. *Chem. Eng. J.* **2022**, *430*, 133157. [[CrossRef](#)]
107. Jia, H.; Shang, N.; Feng, Y.; Ye, H.; Zhao, J.; Wang, H.; Wang, C.; Zhang, Y. Facile preparation of Ni nanoparticle embedded on mesoporous carbon nanorods for non-enzymatic glucose detection. *J. Colloid Interface Sci.* **2021**, *583*, 310–320. [[CrossRef](#)]
108. Abrori, S.A.; Septiani, N.L.W.; Nugraha; Anshori, I.; Suyatman; Suendo, V.; Yulianto, B. Metal-organic-framework FeBDC-derived Fe<sub>3</sub>O<sub>4</sub> for non-enzymatic electrochemical detection of glucose. *Sensors* **2020**, *20*, 4891. [[CrossRef](#)]
109. Wang, L.; Yang, Y.; Wang, B.; Duan, C.; Li, J.; Zheng, L.; Li, J.; Yin, Z. Bifunctional three-dimensional self-supporting multistage structure CC@MOF-74(NiO)@NiCo LDH electrode for supercapacitors and non-enzymatic glucose sensors. *J. Alloys Compd.* **2021**, *885*, 160899. [[CrossRef](#)]
110. Zhang, D.; Wang, Z.; Li, J.; Hu, C.; Zhang, X.; Jiang, B.; Cao, Z.; Zhang, J.; Zhang, R. MOF-derived ZnCo<sub>2</sub>O<sub>4</sub> porous micro-rice with enhanced electro-catalytic activity for the oxygen evolution reaction and glucose oxidation. *RSC Adv.* **2020**, *10*, 9063–9069. [[CrossRef](#)]

111. Li, G.; Xie, G.; Chen, D.; Gong, C.; Chen, X.; Zhang, Q.; Pang, B.; Zhang, Y.; Li, C.; Hu, J.; et al. Facile synthesis of bamboo-like Ni<sub>3</sub>S<sub>2</sub>@NCNT as efficient and stable electrocatalysts for non-enzymatic glucose detection. *Appl. Surf. Sci.* **2022**, *585*, 152683. [[CrossRef](#)]
112. Zhang, C.; Zhang, J.-R.; Han, C.; Zhang, Y.-H.; Yang, S.-H.; Meng, W. Synthesis of Porous CuO Based on an Etching Strategy and Application in Electrochemical Glucose Sensing. *Chin. J. Inorg. Chem.* **2021**, *37*, 2249–2259.
113. Zhang, D.; Zhang, X.; Bu, Y.; Zhang, J.; Zhang, R. Copper cobalt sulfide structures derived from MOF precursors with enhanced electrochemical glucose sensing properties. *Nanomaterials* **2022**, *12*, 1394. [[CrossRef](#)] [[PubMed](#)]
114. Wang, F.; Hu, J.; Liu, Y.; Yuan, G.; Zhang, S.; Xu, L.; Xue, H.; Pang, H. Turning coordination environment of 2D nickel-based metal-organic frameworks by pi-conjugated molecule for enhancing glucose electrochemical sensor performance. *Mater. Today Chem.* **2022**, *24*, 100885. [[CrossRef](#)]
115. Sobhanie, E.; Roshani, A.; Hosseini, M. Microfluidic systems with amperometric and voltammetric detection and paper-based sensors and biosensors. In *Carbon Nanomaterials-Based Sensors*, 1st ed.; Manjunatha, J.G., Hussain, C.M., Eds.; Elsevier: Amsterdam, The Netherlands, 2022; pp. 275–287.
116. Ünlüer, Ö.B.; Ghorbani-Bidkorbeh, F.; Keçili, R.; Hussain, C.M. Future of the modern age of analytical chemistry: Nanominiaturization. In *Handbook on Miniaturization in Analytical Chemistry*, 1st ed.; Hussain, C.M., Ed.; Elsevier: Amsterdam, The Netherlands, 2020; pp. 277–296.
117. Venton, B.J.; DiScenza, D.J. Voltammetry. In *Electrochemistry for Bioanalysis*, 1st ed.; Patel, B., Ed.; Elsevier: Amsterdam, The Netherlands, 2021; pp. 27–50.
118. Foley, M.P.; Du, P.; Griffith, K.J.; Karty, J.A.; Mubarak, M.S.; Raghavachari, K.; Peters, D.G. Electrochemistry of substituted salen complexes of nickel(II): Nickel(I)-catalyzed reduction of alkyl and acetylenic halides. *J. Electroanal. Chem.* **2010**, *647*, 194–203. [[CrossRef](#)]
119. Nandhini, C.; Arul, P.; Huang, S.-T.; Tominaga, M.; Huang, C.-H. Electrochemical sensing of dual biomolecules in live cells and whole blood samples: A flexible gold wire-modified copper-organic framework-based hybrid composite. *Bioelectrochemistry* **2023**, *152*, 108434. [[CrossRef](#)] [[PubMed](#)]
120. Xue, Z.; Jia, L.; Zhu, R.-R.; Du, L.; Zhao, Q.-H. High-performance non-enzymatic glucose electrochemical sensor constructed by transition nickel modified Ni@Cu-MOF. *J. Electroanal. Chem.* **2020**, *858*, 113783. [[CrossRef](#)]
121. Lu, M.; Deng, Y.; Li, Y.; Li, T.; Xu, J.; Chen, S.W.; Wang, J. Core-shell MOF@MOF composites for sensitive nonenzymatic glucose sensing in human serum. *Anal. Chim. Acta* **2020**, *1110*, 35–43. [[CrossRef](#)]
122. Niu, X.; Li, X.; Pan, J.; He, Y.; Qiu, F.; Yan, Y. Recent advances in non-enzymatic electrochemical glucose sensors based on non-precious transition metal materials: Opportunities and challenges. *RSC Adv.* **2016**, *6*, 84893–84905. [[CrossRef](#)]
123. Kim, S.E.; Muthurasu, A. Metal-organic framework-assisted bimetallic Ni@Cu microsphere for enzyme-free electrochemical sensing of glucose. *J. Electroanal. Chem.* **2020**, *873*, 114356. [[CrossRef](#)]
124. Kim, S.E.; Muthurasu, A. Highly Oriented Nitrogen-doped Carbon Nanotube Integrated Bimetallic Cobalt Copper Organic Framework for Non-enzymatic Electrochemical Glucose and Hydrogen Peroxide Sensor. *Electroanalysis* **2021**, *33*, 1333–1345. [[CrossRef](#)]
125. Zoski, C.G. *Handbook of Electrochemistry*; Elsevier Science: Amsterdam, The Netherlands, 2006.
126. Franklin, R.K.; Martin, S.M.; Strong, T.D.; Brown, R.B. Chemical Sensors. In *Comprehensive Microsystems*, 1st ed.; Gianchandani, Y.B., Tabata, O., Zappe, H., Eds.; Elsevier: Oxford, UK, 2008; pp. 433–461.
127. Uzak, D.; Atiroglu, A.; Atiroglu, V.; Cakiroglu, B.; Ozacar, M. Reduced Graphene Oxide/Pt Nanoparticles/Zn-MOF-74 Nanomaterial for a Glucose Biosensor Construction. *Electroanalysis* **2020**, *32*, 510–519. [[CrossRef](#)]
128. Cheng, X.; Zhou, J.; Chen, J.; Xie, Z.; Kuang, Q.; Zheng, L. One-step synthesis of thermally stable artificial multienzyme cascade system for efficient enzymatic electrochemical detection. *Nano Res.* **2019**, *12*, 3031–3036. [[CrossRef](#)]
129. Batista Deroco, P.; Giarola, J.d.F.; Wachholz Júnior, D.; Arantes Lorga, G.; Tatsuo Kubota, L. Paper-based electrochemical sensing devices. In *Comprehensive Analytical Chemistry*, 1st ed.; Merkoçi, A., Ed.; Elsevier: Amsterdam, The Netherlands, 2020; Volume 89, pp. 91–137.
130. Simões, F.R.; Xavier, M.G. Electrochemical Sensors. In *Nanoscience and Its Applications*, 1st ed.; Da Róz, A.L., Ferreira, M., de Lima Leite, F., Oliveira, O.N., Eds.; William Andrew Publishing: Norwich, NY, USA, 2016; pp. 155–178.
131. Song, Y.; Xu, M.; Gong, C.; Shen, Y.; Wang, L.; Xie, Y.; Wang, L. Ratiometric electrochemical glucose biosensor based on GOD/AuNPs/Cu-BTC MOFs/macroporous carbon integrated electrode. *Sens. Actuators B Chem.* **2018**, *257*, 792–799. [[CrossRef](#)]
132. Clark, L.C., Jr.; Lyons, C. Electrode systems for continuous monitoring in cardiovascular surgery. *Ann. N. Y. Acad. Sci.* **1962**, *102*, 29–45. [[CrossRef](#)] [[PubMed](#)]
133. Adeloju, S.B. AMPEROMETRY. In *Encyclopedia of Analytical Science*, 2nd ed.; Worsfold, P., Townshend, A., Poole, C., Eds.; Elsevier: Oxford, UK, 2005; pp. 70–79.
134. Chu, C.; Rao, S.; Ma, Z.; Han, H. Copper and cobalt nanoparticles doped nitrogen-containing carbon frameworks derived from CuO-encapsulated ZIF-67 as high-efficiency catalyst for hydrogenation of 4-nitrophenol. *Appl. Catal. B* **2019**, *256*, 117792. [[CrossRef](#)]
135. Zhai, Z.; Wang, J.; Sun, Y.; Hao, X.; Niu, B.; Xie, H.; Li, C. MOFs/nanofiber-based capacitive gas sensors for the highly selective and sensitive sensing of trace SO<sub>2</sub>. *Appl. Surf. Sci.* **2023**, *613*, 155772. [[CrossRef](#)]

136. Mo, G.; Zheng, X.; Ye, N.; Ruan, Z. Nitrogen-doped carbon dodecahedron embedded with cobalt nanoparticles for the direct electro-oxidation of glucose and efficient nonenzymatic glucose sensing. *Talanta* **2021**, *225*, 121954. [[CrossRef](#)]
137. Wang, L.; Miao, X.; Qu, Y.; Duan, C.; Wang, B.; Yu, Q.; Gao, J.; Song, D.; Li, Y.; Yin, Z. Rattle-type Au@NiCo LDH hollow core-shell nanostructures for nonenzymatic glucose sensing. *J. Electroanal. Chem.* **2020**, *858*, 113810. [[CrossRef](#)]
138. Zhang, L.; Wang, J.; Ren, X.; Zhang, W.; Zhang, T.; Liu, X.; Du, T.; Li, T.; Wang, J. Internally extended growth of core-shell NH<sub>2</sub>-MIL-101(Al)@ZIF-8 nanoflowers for the simultaneous detection and removal of Cu(II). *J. Mater. Chem. A* **2018**, *6*, 21029–21038. [[CrossRef](#)]
139. Heller, A.; Feldman, B. Electrochemical Glucose Sensors and Their Applications in Diabetes Management. *Chem. Rev.* **2008**, *108*, 2482–2505. [[CrossRef](#)] [[PubMed](#)]
140. Witkowska Nery, E.; Kundys, M.; Jeleń, P.S.; Jönsson-Niedziółka, M. Electrochemical Glucose Sensing: Is There Still Room for Improvement? *Anal. Chem.* **2016**, *88*, 11271–11282. [[CrossRef](#)] [[PubMed](#)]
141. Shu, Y.; Su, T.; Lu, Q.; Shang, Z.; Xu, Q.; Hu, X. Highly Stretchable Wearable Electrochemical Sensor Based on Ni-Co MOF Nanosheet-Decorated Ag/rGO/PU Fiber for Continuous Sweat Glucose Detection. *Anal. Chem.* **2021**, *93*, 16222–16230. [[CrossRef](#)]
142. Sun, L.; Hendon, C.H.; Park, S.S.; Tulchinsky, Y.; Wan, R.; Wang, F.; Walsh, A.; Dincă, M. Is iron unique in promoting electrical conductivity in MOFs? *Chem. Sci.* **2017**, *8*, 4450–4457. [[CrossRef](#)] [[PubMed](#)]
143. Xuan, X.; Qian, M.; Pan, L.; Lu, T.; Han, L.; Yu, H.; Wan, L.; Niu, Y.; Gong, S. A longitudinally expanded Ni-based metal-organic framework with enhanced double nickel cation catalysis reaction channels for a non-enzymatic sweat glucose biosensor. *J. Mater. Chem. B* **2020**, *8*, 9094–9109. [[CrossRef](#)]
144. Chen, Y.; Tian, Y.; Zhu, P.; Du, L.; Chen, W.; Wu, C. Electrochemically Activated Conductive Ni-Based MOFs for Non-enzymatic Sensors Toward Long-Term Glucose Monitoring. *Front. Chem.* **2020**, *8*, 602752. [[CrossRef](#)]
145. Sun, Y.; Li, Y.; Wang, N.; Xu, Q.Q.; Xu, L.; Lin, M. Copper-based Metal-organic Framework for Non-enzymatic Electrochemical Detection of Glucose. *Electroanalysis* **2018**, *30*, 474–478. [[CrossRef](#)]
146. Hu, Q.; Qin, J.; Wang, X.F.; Ran, G.Y.; Wang, Q.; Liu, G.X.; Ma, J.P.; Ge, J.Y.; Wang, H.Y. Cu-Based Conductive MOF Grown in situ on Cu Foam as a Highly Selective and Stable Non-Enzymatic Glucose Sensor. *Front. Chem.* **2021**, *9*, 786970. [[CrossRef](#)]
147. Kim, K.; Kim, S.; Lee, H.N.; Park, Y.M.; Bae, Y.-S.; Kim, H.-J. Electrochemically derived CuO nanorod from copper-based metal-organic framework for non-enzymatic detection of glucose. *Appl. Surf. Sci.* **2019**, *479*, 720–726. [[CrossRef](#)]
148. Wang, Z.; Liu, T.; Yu, Y.; Asif, M.; Xu, N.; Xiao, F.; Liu, H. Coffee Ring-Inspired Approach toward Oriented Self-Assembly of Biomimetic Murray MOFs as Sweat Biosensor. *Small* **2018**, *14*, e1802670. [[CrossRef](#)]
149. Ezzati, M.; Shahrokhian, S.; Hosseini, H. In Situ Two-Step Preparation of 3D NiCo-BTC MOFs on a Glassy Carbon Electrode and a Graphitic Screen Printed Electrode as Nonenzymatic Glucose-Sensing Platforms. *ACS Sustain. Chem. Eng.* **2020**, *8*, 14340–14352. [[CrossRef](#)]
150. Zhang, L.; Wang, N.; Cao, P.; Lin, M.; Xu, L.; Ma, H. Electrochemical non-enzymatic glucose sensor using ionic liquid incorporated cobalt-based metal-organic framework. *Microchem. J.* **2020**, *159*, 105343. [[CrossRef](#)]
151. Chen, C.; Xu, H.; Zhan, Q.; Zhang, Y.; Wang, B.; Chen, C.; Tang, H.; Xie, Q. Preparation of novel HKUST-1-glucose oxidase composites and their application in biosensing. *Microchim. Acta* **2022**, *190*, 10. [[CrossRef](#)] [[PubMed](#)]
152. Kumar, R.; Chauhan, S. Nano/micro-scaled materials based optical biosensing of glucose. *Ceram. Int.* **2022**, *48*, 2913–2947. [[CrossRef](#)]
153. Guo, J.; Liu, Y.; Mu, Z.; Wu, S.; Wang, J.; Yang, Y.; Zhao, M.; Wang, Y. Label-free fluorescence detection of hydrogen peroxide and glucose based on the Ni-MOF nanozyme-induced self-ligand emission. *Microchim. Acta* **2022**, *189*, 219. [[CrossRef](#)]
154. Zhong, X.; Xia, H.; Huang, W.; Li, Z.; Jiang, Y. Biomimetic metal-organic frameworks mediated hybrid multi-enzyme mimic for tandem catalysis. *Chem. Eng. J.* **2020**, *381*, 122758. [[CrossRef](#)]
155. Shi, M.-Y.; Xu, M.; Gu, Z.-Y. Copper-based two-dimensional metal-organic framework nanosheets as horseradish peroxidase mimics for glucose fluorescence sensing. *Anal. Chim. Acta* **2019**, *1079*, 164–170. [[CrossRef](#)]
156. Ning, D.; Liu, Q.; Wang, Q.; Du, X.-M.; Ruan, W.-J.; Li, Y. Luminescent MOF nanosheets for enzyme assisted detection of H<sub>2</sub>O<sub>2</sub> and glucose and activity assay of glucose oxidase. *Sens. Actuators B Chem.* **2019**, *282*, 443–448. [[CrossRef](#)]
157. Cui, Y.; Chen, F.; Yin, X.-B. A ratiometric fluorescence platform based on boric-acid-functional Eu-MOF for sensitive detection of H<sub>2</sub>O<sub>2</sub> and glucose. *Biosens. Bioelectron.* **2019**, *135*, 208–215. [[CrossRef](#)]
158. Li, D.; Zhang, S.; Feng, X.; Yang, H.; Nie, F.; Zhang, W. A novel peroxidase mimetic Co-MOF enhanced luminol chemiluminescence and its application in glucose sensing. *Sens. Actuators B Chem.* **2019**, *296*, 126631. [[CrossRef](#)]
159. Jiang, G.; Yang, Z.; Zhu, K.; Zong, S.; Wu, L.; Wang, Z.; Cui, Y. Universal peroxidase-like strategy for sensitive glucose detection in complex matrix. *Nano Res.* **2023**, *16*, 1141–1148. [[CrossRef](#)]
160. Guo, L.; Chen, S.; Yu, Y.-L.; Wang, J.-H. A Smartphone Optical Device for Point-of-Care Testing of Glucose and Cholesterol Using Ag NPs/UiO-66-NH<sub>2</sub>-Based Ratiometric Fluorescent Probe. *Anal. Chem.* **2021**, *93*, 16240–16247. [[CrossRef](#)] [[PubMed](#)]
161. Pan, Y.; Pang, Y.; Shi, Y.; Zheng, W.; Long, Y.; Huang, Y.; Zheng, H. One-pot synthesis of a composite consisting of the enzyme ficin and a zinc(II)-2-methylimidazole metal organic framework with enhanced peroxidase activity for colorimetric detection for glucose. *Microchim. Acta* **2019**, *186*, 213. [[CrossRef](#)]
162. Ilacas, G.C.; Basa, A.; Nelms, K.J.; Sosa, J.D.; Liu, Y.; Gomez, F.A. Paper-based microfluidic devices for glucose assays employing a metal-organic framework (MOF). *Anal. Chim. Acta* **2019**, *1055*, 74–80. [[CrossRef](#)]

163. Hong, J.I.; Chang, B.Y. Development of the smartphone-based colorimetry for multi-analyte sensing arrays. *Lab Chip* **2014**, *14*, 1725–1732. [[CrossRef](#)]
164. Wu, T.; Gao, X.-J.; Ge, F.; Zheng, H.-G. Metal–organic frameworks (MOFs) as fluorescence sensors: Principles, development and prospects. *CrystEngComm* **2022**, *24*, 7881–7901. [[CrossRef](#)]
165. Gui, R.; Jin, H.; Bu, X.; Fu, Y.; Wang, Z.; Liu, Q. Recent advances in dual-emission ratiometric fluorescence probes for chemo/biosensing and bioimaging of biomarkers. *Coord. Chem. Rev.* **2019**, *383*, 82–103. [[CrossRef](#)]
166. Hirano, T.; Matsushashi, C. A stable chemiluminophore, adamantylideneadamantane 1,2-dioxetane: From fundamental properties to utilities in mechanochemistry and soft crystal science. *J. Photochem. Photobiol. C* **2022**, *51*, 100483. [[CrossRef](#)]
167. Zheng, Z.; Cong, S.; Gong, W.; Xuan, J.; Li, G.; Lu, W.; Geng, F.; Zhao, Z. Semiconductor SERS enhancement enabled by oxygen incorporation. *Nat. Commun.* **2017**, *8*, 1993. [[CrossRef](#)]
168. Sun, H.; Yu, B.; Pan, X.; Zhu, X.; Liu, Z. Recent progress in metal–organic frameworks-based materials toward surface-enhanced Raman spectroscopy. *Appl. Spectrosc. Rev.* **2022**, *57*, 513–528. [[CrossRef](#)]
169. Xue, Q.; Li, Z.; Wang, Q.; Pan, W.; Chang, Y.; Duan, X. Nanostrip flexible microwave enzymatic biosensor for noninvasive epidermal glucose sensing. *Nanoscale Horiz.* **2020**, *5*, 934–943. [[CrossRef](#)] [[PubMed](#)]
170. Bandodkar, A.J.; Gutruf, P.; Choi, J.; Lee, K.; Sekine, Y.; Reeder, J.T.; Jeang, W.J.; Aranyosi, A.J.; Lee, S.P.; Model, J.B.; et al. Battery-free, skin-interfaced microfluidic/electronic systems for simultaneous electrochemical, colorimetric, and volumetric analysis of sweat. *Sci. Adv.* **2019**, *5*, eaav3294. [[CrossRef](#)]
171. Zhao, H.; Su, R.; Teng, L.; Tian, Q.; Han, F.; Li, H.; Cao, Z.; Xie, R.; Li, G.; Liu, X.J.N. Recent advances in flexible and wearable sensors for monitoring chemical molecules. *Nanoscale* **2022**, *14*, 1653–1669. [[CrossRef](#)] [[PubMed](#)]
172. Sun, H.; Saeedi, P.; Karuranga, S.; Pinkepank, M.; Ogurtsova, K.; Duncan, B.B.; Stein, C.; Basit, A.; Chan, J.C.N.; Mbanya, J.C.; et al. IDF Diabetes Atlas: Global, regional and country-level diabetes prevalence estimates for 2021 and projections for 2045. *Diabetes Res. Clin. Pr.* **2022**, *183*, 109119. [[CrossRef](#)] [[PubMed](#)]
173. Shao, Z.; Chen, J.; Xie, Q.; Mi, L. Functional metal/covalent organic framework materials for triboelectric nanogenerator. *Coord. Chem. Rev.* **2023**, *486*, 215118. [[CrossRef](#)]
174. Barsiwal, S.; Babu, A.; Khanapuram, U.K.; Potu, S.; Madathil, N.; Rajaboina, R.K.; Mishra, S.; Divi, H.; Kodali, P.; Nagapuri, R.; et al. ZIF-67-Metal-Organic-Framework-Based Triboelectric Nanogenerator for Self-Powered Devices. *Nanoenergy Adv.* **2022**, *2*, 291–302. [[CrossRef](#)]
175. Yang, T.; Yu, X.; Ma, N.; Wu, R.; Li, H. An autonomous channel deep learning framework for blood glucose prediction. *Appl. Soft Comput.* **2022**, *120*, 108636. [[CrossRef](#)]
176. Zhu, T.; Kuang, L.; Daniels, J.; Herrero, P.; Li, K.; Georgiou, P. IoMT-Enabled Real-Time Blood Glucose Prediction With Deep Learning and Edge Computing. *IEEE Internet Things J.* **2023**, *10*, 3706–3719. [[CrossRef](#)]
177. Wu, K.; He, X.; Wang, J.; Pan, T.; He, R.; Kong, F.; Cao, Z.; Ju, F.; Huang, Z.; Nie, L. Recent progress of microfluidic chips in immunoassay. *Front. Bioeng. Biotechnol.* **2022**, *10*, 1112327. [[CrossRef](#)]
178. Martinez, A.W.; Phillips, S.T.; Butte, M.J.; Whitesides, G.M. Patterned Paper as a Platform for Inexpensive, Low-Volume, Portable Bioassays. *Angew. Chem. Int. Ed.* **2007**, *119*, 1340–1342. [[CrossRef](#)]
179. Liu, H.; Crooks, R.M. Paper-Based Electrochemical Sensing Platform with Integral Battery and Electrochromic Read-Out. *Anal. Chem.* **2012**, *84*, 2528–2532. [[CrossRef](#)] [[PubMed](#)]
180. Choi, J.; Bandodkar, A.J.; Reeder, J.T.; Ray, T.R.; Turnquist, A.; Kim, S.B.; Nyberg, N.; Hourlier-Fargette, A.; Model, J.B.; Aranyosi, A.J.; et al. Soft, Skin-Integrated Multifunctional Microfluidic Systems for Accurate Colorimetric Analysis of Sweat Biomarkers and Temperature. *ACS Sens.* **2019**, *4*, 379–388. [[CrossRef](#)] [[PubMed](#)]

**Disclaimer/Publisher’s Note:** The statements, opinions and data contained in all publications are solely those of the individual author(s) and contributor(s) and not of MDPI and/or the editor(s). MDPI and/or the editor(s) disclaim responsibility for any injury to people or property resulting from any ideas, methods, instructions or products referred to in the content.